PHILOSOPHICAL TRANSACTIONS OF THE ROYAL SOCIETY A MATHEMATICAL, PHYSICAL & ENGINEERING SCIENCES

Measurements of the Viscometric Functions for a Fluid in Steady Shear Flows

W. G. Pritchard

Phil. Trans. R. Soc. Lond. A 1971 **270**, 507-556
doi: 10.1098/rsta.1971.0088

MEASUREMENTS OF THE VISCOMETRIC FUNCTIONS FOR A FLUID IN STEADY SHEAR FLOWS

By W. G. PRITCHARD†

Department of Chemical Engineering and Rheology Research Center, University of Wisconsin, Madison, Wisconsin 53706

(*Communicated by T. B. Benjamin, F.R.S.—Received* 11 *March* 1971)

CONTENTS

	PAGE
1. Introduction	508
2. Theoretical aspects	510
2.1. The cone-and-plate viscometer	511
2.2. Torsional flow between parallel plates	514
2.3. Flow between concentric cylinders	515
2.4. Stress-optical methods	516
3. Experimental apparatus	517
4. Preparation and stability of the liquid	521
4.1. Preparation	521
4.2. Stability	522
5. Measurements of the shear-stress function	523
6. The primary normal-stress difference	525
7. The normal-stress distribution $p_{22}(r)$	528
8. The error arising from the holes	532
8.1. Determination of $p_H(\dot{s})$	532
8.2. The normal stress at the rim	535
8.3. Concentric-cylinders measurements	537
9. The secondary normal-stress difference	540
9.1. The Jackson & Kaye method	541
9.2. The Marsh & Pearson method	542
9.3. The Kotaka *et al.* method	543
9.4. Discussion	544
10. In conclusion	546
Appendixes	548
A. The intrinsic error in the use of a cavity to measure p_{22}	548
B. The test used by Markovitz (1965*a*)	551
C. The influence of the sea of liquid on $\bar{p}(R)$	552
D. An estimate of the secondary normal-stress difference	553
References	555

This paper describes a series of experiments in which the three material functions of steady viscometric flows were measured for a given polyisobutene solution. A number of instruments and measuring techniques were used in order to check the experimental method.

The shear stress was determined from the torque transmitted by the fluid in a cone-and-plate apparatus and in Couette flow between concentric cylinders. The results obtained from these measurements were in good agreement with each other.

The primary normal-stress difference was determined from the normal force acting on the plate of a cone-and-plate apparatus, and from stress-optical measurements on Couette flow between concentric cylinders. These results are in good agreement with each other. Detailed measurements of the distribution

† Permanent address: Fluid Mechanics Research Institute, University of Essex, Colchester, Essex.

Vol. 270. A. 1208. (Price £1.30; U.S. $3.40) 38 [Published 2 December 1971]

of the normal stress acting on the plate of the cone-and-plate apparatus were made for three cone angles and for two boundary configurations at the rim of the apparatus: from these results a combination of the primary and the secondary normal-stress differences was deduced, thereby making possible the computation of the secondary normal-stress difference.

When the normal stress acting on a rigid surface is measured by means of a hole leading to a pressure transducer the results are in error by an amount roughly proportional to the primary normal-stress difference of the fluid (cf. Kaye, Lodge & Vale 1968). In the present experiments this error was determined from measurements of the distribution of the normal stress acting on the plates of a plate-and-plate apparatus, together with the assumption that the error is a function only of the shear rate at the position of the hole in the undisturbed viscometric flow. The values of the measuring error thus obtained are in good agreement with measurements made in Couette flow between concentric cylinders.

The secondary normal-stress difference, P_2, was measured in a number of different ways. From the results it is suggested that the methods of Jackson & Kaye and of Marsh & Pearson may be imprecise and, in particular, may yield incorrect values for P_2. A new, direct, method of estimating P_2, suggested by Higashitani & Pritchard (1971) and outlined in appendix A, may provide a more convenient means of determining P_2.

1. Introduction

The measurements described herein are the results of an extensive series of experiments aimed at determining the material functions for viscometric flows of a given polymer solution. The experiments have been carried out on a number of different instruments, and by a number of different experimenters, in an attempt to isolate any discrepancies or any sources of error among the measurements. In many respects this work is similar to a set of measurements conducted by Professor A. S. Lodge, the major part of which is described by Kaye, Lodge & Vale (1968); but since experience suggests that extreme caution is needed with experiments on highly nonlinear fluids, we have in the main followed the previous experiments, but with the present fluid we have made a far more detailed and comprehensive set of measurements than hitherto.

When investigating the rheological properties of liquids it is usually assumed that the liquid is homogeneous, isotropic and incompressible, and that the forces acting within the body of the fluid can be described by a symmetric stress-tensor field, $\boldsymbol{p}$. If a further assumption is made that the value of the stress tensor at a given point in the fluid is determined, to within an additive isotropic pressure, by the shape history of a small element surrounding that point there results a class of rheological equations of state considered by Oldroyd (1950), a class which includes (see Lodge & Stark 1970) the *simple fluid* defined by Noll (1958).† Thus, for isothermal motions of these fluids,‡ the stress at a given time t is related to the strain history by some operator $\mathscr{F}$, so that

$$\overset{t}{\underset{t'=-\infty}{\mathscr{F}}} \{(\boldsymbol{p})_t, \underset{t'\to t}{\text{strain}}\} = 0. \tag{1.1}$$

If, however, we restrict our attention to a particular class of steady shear flows, called viscometric flows, in which the shear rate at a particle is a constant in time, the operator $\mathscr{F}$ is greatly simplified and becomes an ordinary function. All viscometric flows of a simple fluid may be characterized completely by the three material functions p_{21}, $p_{11}-p_{22}$ and $p_{22}-p_{33}$ (where the p_{ij} are the physical components of the stress tensor, $\boldsymbol{p}$), which are functions only of the local shear rate (see Coleman & Noll 1959; Lodge 1964, p. 343). It is an inevitable consequence of the simple-fluid assumption that the three material functions are independent of the kind of viscometric flow in which they are measured and are completely determined by the local shear rate. Hence in view of the extreme difficulties of verifying experimentally the basic assumptions underlying the theory, this

† In this paper we shall use the term 'simple fluid' to refer to the class of fluids defined by Oldroyd.

‡ It is assumed throughout this paper that heat generation and temperature variations are negligible.

corollary provides an indirect check of the assumptions. On the other hand, given a sample of a simple fluid, it is of interest to know which are the easiest and most reliable methods of determining the material functions for viscometric flows. To date only two experimental determinations of the material functions have been made in which sufficient measurements were carried out to check the reliability of the results. One set of measurements by Markovitz (1965*a*) (and see in Coleman, Markovitz & Noll 1966) determined the two normal-stress differences from the following:

(*a*) The measurement of the difference in the stress p_{22}† in Couette flow between two concentric cylinders. This should give a direct measure of $p_{11}-p_{22}$.

(*b*) The gradient of the stress p_{22} acting on the plate of a cone-and-plate viscometer. This gives a measure of the combination $p_{11}+p_{22}-2p_{33}$.

By using these two sets of results it is possible to make a prediction of the stress p_{22} acting on the plates of a plate-and-plate viscometer, and Markovitz found such a prediction to agree extremely well with the measured values. However, in the experiments described herein, agreement has not been attained with this test, and it would appear that Markovitz's result is anomalous.

The other detailed experimental check of the internal consistency of various measurements of the material functions has, as already indicated, been carried out by Professor A. S. Lodge, and the main results of this work are described in Kaye *et al.* (1968). It was found that agreement among the various estimates of $p_{11}-p_{22}$ and $p_{22}-p_{33}$ could not be attained unless a systematic error was introduced arising from the use of 'small' holes to measure the stress p_{22}. (In these experiments estimates of p_{22} were made by assuming it to be equal to the normal stress acting at the bottom of a cavity in the wall of the viscometer, rather than making the measurement at the wall itself). The introduction of this so-called 'hole effect' explained all their experimental discrepancies, except for one estimate of $p_{22}-p_{33}$, which is discussed below. Thus Kaye *et al.* suggest that estimates of p_{22} made from stress measurements at the bottom of a cavity in the surface of a viscometer give rise to important errors (about 0.2 $(p_{11}-p_{22})$ in magnitude for their fluid), and that the error depends only on the shear rate in the undisturbed fluid at the wall of the viscometer. More recent work by Tanner & Pipkin (1969) and by Pritchard (1970) has proposed an explanation of this phenomenon, and Tanner & Pipkin were able to show for slow, two-dimensional, flows of a second-order fluid, that the magnitude of the error p_{H} in the estimate of p_{22} is $\frac{1}{4}(p_{11}-p_{22})$, when the hole is very deep and symmetrical. Physically the error arises because of an additional local curvature imposed on the streamlines of the basic, viscometric, flow by the presence of the cavity. We have already mentioned for the case of Couette flow between concentric cylinders that the difference in p_{22} across the gap is a measure of the normal-stress difference $p_{11}-p_{22}$; thus, in a similar fashion, the fluid flow within the cavity gives rise to a value of p_{22} at the bottom of the cavity which is different from that at the opening of the cavity, and at the wall of the viscometer, and this difference is directly related to $p_{11}-p_{22}$.‡ Moreover, for slow, two-dimensional, flows of a Newtonian fluid it follows that no error is introduced when p_{22} is measured in this way. An interesting outcome of these arguments is that, for very deep and symmetrical holes, the measured value of p_{22} is completely independent of the actual shape of the cavity. This result is strictly applicable only for second-order fluids, yet the experiments of Pritchard (1970) indicate, for a fluid for which the second-order approximation is *not* valid, that the measured value of p_{22}

† Throughout the paper we use the terminology of Lodge (1964). Thus, with respect to the orthogonal curvilinear coordinate system (x^1, x^2, x^3), the shear flow under consideration is $(v^1(x^2), 0, 0)$, where $\boldsymbol{v}$ is the velocity.

‡ This argument is described in more detail in appendix A.

PHILOSOPHICAL TRANSACTIONS OF THE ROYAL SOCIETY A MATHEMATICAL, PHYSICAL & ENGINEERING SCIENCES

(for deep cavities and for a given shear rate at the wall of the viscometer) is independent of a very wide range of cavity shapes.

In their experiments Kaye *et al.* (1968) were able to make an independent check of the measuring error, p_H, which confirmed their hypothesis. Thus, in summary, Kaye *et al.* made two separate measurements of $p_{11}-p_{22}$ and of p_{21}, both measurements of each quantity being in agreement; two estimates of p_H, which are in good agreement; and two measurements of $p_{22}-p_{33}$, which are *not* in agreement with each other, but it is possible that this difference could be attributed to experimental inaccuracies rather than to a systematic discrepancy.

One of the reasons for undertaking the present measurements was to attempt to confirm, using a slightly different liquid, the findings of Kaye *et al.* (1968). In view of the unexpected results one can often obtain with non-Newtonian fluids it was felt that such a check would be of value. Moreover, with these new measurements, it has been possible to investigate in a fair amount of detail a number of methods of determining $p_{22}-p_{33}$ in an attempt to explain, or to confirm, the remaining inconsistency noted by Kaye *et al.* (1968). Unfortunately it has not been possible to resolve this disagreement, in that similar discrepancies have been found once again; these anomalies cannot be accounted for.

Because of the large number of possible sources of error involved with the present measurements we have tried, in this paper, to give a fairly detailed account of the whole experiment, rather than err on the side of terseness. Thus, in addition to the main corpus of the work carried out in Manchester there are also presented, for comparison, the results of measurements on the same fluid made on two commercially produced rheogoniometers.

2. Theoretical aspects

The theory of viscometric flows of simple fluids has been discussed in detail by many authors (see, for example Lodge 1964; Coleman *et al.* 1966) and hence in this section we discuss briefly only the results of direct relevance to the experiments. The notation of Lodge (1964) is used throughout.

As indicated in the introduction, a viscometric flow is one for which the rate of shear at a particle is a constant for the entire history of the fluid. Thus a steady flow belongs to the class of viscometric flows if an orthogonal curvilinear coordinate system (x^1, x^2, x^3) can be found such that the contravariant components of the velocity field, with respect to the system, are $(v^1(x^2), 0, 0)$.† Of course these flows must be dynamically admissible, in the sense that the velocity field and the stress distribution satisfy the equations of motion.‡ Accordingly some examples of viscometric flows are: Couette flow between concentric cylinders; Poiseuille flow; and, neglecting inertial effects, flows in cone-and-plate and plate-and-plate viscometers (however the viscometric flow between a cone and a plate is dynamically admissible only in the limit of very small cone angles). We shall discuss herein experiments made with each one of these flows.

But the basis of the theory lies in the simple-fluid assumptions, namely that the fluid is homogeneous, isotropic and incompressible; that the forces acting within the fluid may be described by a symmetric stress-tensor field, $\boldsymbol{p}$; and that the value of the stress tensor at a point in the fluid is determined, to within an additive isotropic pressure, by the shape history of a small element

† This description of viscometric flows is not exhaustive, though it includes most of the viscometric flows and certainly all the flows we shall consider herein. A complete description is given by Coleman *et al.* (1966) and by Pipkin (1968).

‡ It is assumed that there is no slip between the fluid and a solid surface.

surrounding that point. The definitions of homogeneity and isotropy are interrelated and are probably most easily described in the way discussed by Oldroyd (1950) (and see Lodge 1964, p. 331). Oldroyd describes the stress tensor at a point in terms of a convected coordinate system, in which the coordinate surfaces ξ^i = constant are chosen as surfaces drawn in the material (and deforming continuously with it), and the ξ^i and the time t are taken as independent variables. This procedure avoids any dependence on the absolute motion in space of a material element, or on the conditions in other material elements. Thus, with respect to this coordinate system, there will arise in (1.1) a set of physical constants describing the particular material under consideration. These quantities are strictly constant tensors associated with the material in the 'small element' containing the particle ξ^i (and are invariant in time). Now, the material is said to be *isotropic* if these physical constants are expressible as scalar body fields (together with the body metric field if necessary). A *homogeneous* material is one in which the physical constants may be described by body fields whose covariant derivative (formed with the use of the body metric tensor) is zero. Accordingly an isotropic material which is homogeneous in one state, say a rest configuration, is homogeneous for all time: the material constants are described by scalar fields and hence the covariant derivative reduces to the partial derivative $\partial/\partial\xi^i$ and is independent of the body metric tensor.

The symmetry of the stress tensor follows from the conservation of angular momentum, *if we assume there are no couple stresses within the body of the fluid*. There is no physical reason *a priori* why this assumption should be valid, but in view of its success in other areas of continuum mechanics we shall retain it until forced to reconsider.

The assumption that the stress tensor at a point in the fluid is determined by the shape history of a small material element surrounding that point is crucial. Materials for which this is not valid, in that the stress tensor is influenced by neighbouring material elements,† are usually termed *non-simple* or *complex* fluids. On a continuum or macroscopic basis the so-called 'material elements' are, in some sense, infinitesimally small; but from a physical viewpoint they must be sufficiently large that statistical averages, made on a molecular basis, are independent of the volume of the chosen element. To indicate the kind of length scales influencing these considerations it is worth noting that the radius of gyration of the (high molecular weight) polymer molecules used in the current experiments is of the order of 0.1 μm, but this figure may be somewhat misleading when the solutions are so concentrated that the polymer coils become extensively intertwined.

We shall now consider the actual stress distributions arising in the viscometers used in the experiments.

2.1. *The cone-and-plate viscometer*

(*a*) *Introductory comments*

We consider a cone of radius R to be rotating about its axis at a uniform angular velocity Ω; the apex of the cone is a distance c above a stationary flat plate, as indicated in the sketch of figure 1*a*.‡ For this geometric arrangement the conical surfaces $z = k(c + r\tan\beta)$, $0 \leqslant k \leqslant 1$, are assumed to rotate effectively as rigid surfaces with a constant angular velocity about the axis; r is the radius from the axis. Apart from a region near the rim of the cone, Marsh & Pearson (1968) have pointed out, on the basis of a lubrication approximation (see Pearson 1967), that this flow is viscometric,

† An example of such a fluid is one whose rheological equations of state include covariant derivatives at the time t of the body stress tensor or the body metric tensor at time t'.

‡ Although it is not shown in figure 1, the apex of each cone used in the current experiments had been ground off and hence it was possible to use some negative values of c. These truncations obviously introduce an error to the experiments, and we shall discuss this below.

at least in the asymptotic limit of small cone angles (β), and for small values of the parameter c/R. Having thus prescribed a velocity field in the viscometer we must verify that it is admissible in that it satisfies the equations of motion and continuity. The continuity condition is satisfied identically by the velocity field, but the equations of motion are satisfied only under the following conditions:

(i) That inertial effects are negligible, the so-called slow-flow approximation. The largest Reynolds number arising in these experiments, based on the velocity and the gap width at the rim of the viscometer, is about 0.01.†

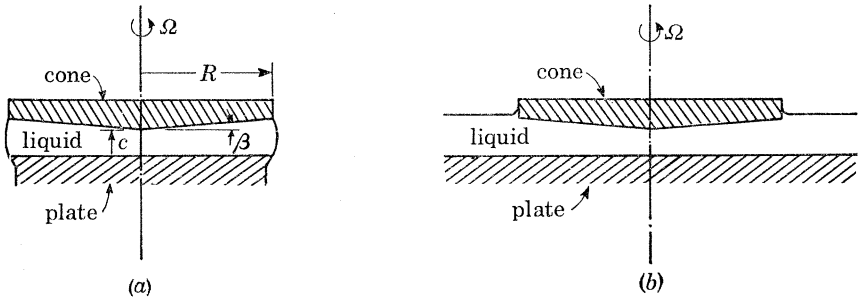

FIGURE 1. Schematic diagram of the cone-and-plate viscometer. (*a*) A configuration of the liquid referred to as the 'free-boundary state'; (*b*) an alternative arrangement referred to as a 'sea of liquid'.

(ii) That the boundary conditions at the liquid/air interface are satisfied without the introduction of secondary flows. In general this is not possible and hence the two kinds of interface shown in figure 1 have been used to investigate the importance of this assumption.‡

(iii) That terms in the equations of motion of order $\tan^2\beta$ (separate terms in the relation being of order 1) may be neglected (see Coleman *et al.* (1966), and Marsh & Pearson (1968) for details of this approximation). We shall check the importance of this effect by making measurements with cones of differing angles.§

Having made these assumptions it follows that the distribution of normal stresses acting on the plate satisfies the relation (see Marsh & Pearson 1968)

$$\frac{\partial p_{33}}{\partial r} = \frac{p_{11}-p_{33}}{r} + \frac{\tan\beta(p_{22}-p_{33})}{c+r\tan\beta}, \tag{2.1}$$

† Kaye (1965) has made an approximate analysis of this inertial correction for the case of a Newtonian fluid in a cone-and-plate viscometer. Assuming the resultant secondary flows are much smaller in magnitude than the primary flow Kaye estimates that this secondary flow makes a contribution to the stress p_{22} of magnitude $\frac{3}{20}\rho r^2\Omega^2$. The largest value of this quantity, in any of the experiments, is 8 dyn/cm² which is less than 0.1 % of the value measured in that experiment. If this correction were applied it would *increase* the estimate of $p_{11}+p_{22}-2p_{33}$ (see (2.4), to follow) and would reduce the estimate of $p_{11}-p_{22}$ (see (2.6)). A contribution to p_{22} also arises from the centrifugal forces in the rotating liquid (see Walters & Waters 1968; Adams & Lodge 1964); this contribution is also of negligible importance in the present measurements.

‡ The errors introduced by the secondary flows generated near the rim are difficult to calculate theoretically, however Griffiths & Walters (1970) have made an estimate of their magnitudes for the sea-of-liquid configuration. Their calculation is for a second-order fluid and the upper surface of the cone is assumed to form part of a sphere. For the particular fluid chosen by Griffiths & Walters it is estimated that the error in the normal force on the plate, arising from the unwanted secondary flows, is less than 0.1 % when the cone angle $\beta < 4°$: they accordingly conclude that both the normal-stress distribution and total force measurements for determining normal-stress differences are not likely to be unduly affected by edge effects.

§ For a second-order fluid Kaye (1965) has made an estimate of the correction to p_{22} arising from this source. The calculations suggest, for small cone angles, that the correction varies as the logarithm of the radius and hence would lead to a systematic error, dependent only on the cone angle, in our estimate of $p_{11}+p_{22}-2p_{33}$ (cf. (2.4)). The ratio of this correction to the primary term of p_{22} is only $\frac{3}{5}\beta^2$: thus for the 5.67° cone there would be an error of 0.57 % in the estimate of $p_{11}+p_{22}-2p_{33}$; for the 3.26° cone the error is 0.19 %. If a correction of this kind were made it would *reduce* our estimate of $p_{11}+p_{22}-2p_{33}$.

with the boundary condition at the rim of the cone assumed to be

$$p_{33}(R) = 0. \tag{2.2}$$

(The ambient pressure may be chosen to be zero without loss of generality.) The shear rate $\dot{s}$ at the radius r is

$$\dot{s} = \frac{\Omega r}{c + r\tan\beta}, \tag{2.3}$$

where Ω denotes the angular velocity of the cone.

(*b*) *The configuration with* $c = 0$

When the tip of the cone just touches the plate, so that $c = 0$, we see from (2.3) that the shear rate is independent of the radius. Accordingly the normal-stress difference $p_{22} - p_{33}$ is also independent of the radius, so that $\partial p_{22}/\partial r = \partial p_{33}/\partial r$, whence (2.1) may be written in the form

$$r\,\partial p_{22}/\partial r = P_1 + 2P_2 \quad (c = 0). \tag{2.4}$$

In (2.4) we have introduced the symbols P_1 for the primary normal-stress difference $p_{11} - p_{22}$, and P_2 for the secondary normal-stress difference $p_{22} - p_{33}$. Since P_1 and P_2 are functions only of the shear rate (2.4) implies that the normal stress p_{22}, acting on the plate, varies logarithmically with the radius. Moreover, since P_2 is independent of the radius, it follows from the boundary condition (2.2) that

$$p_{22}(R) = P_2. \tag{2.5}$$

Then using the condition (2.5), and integrating p_{22} over the area of the plate, we find that, as a result of the shear flow of the liquid, the total normal force F acting on the plate is

$$F = \tfrac{1}{2}\pi R^2 P_1. \tag{2.6}$$

(All the cones used in the current experiments had been truncated at their vertices. Typically this would mean the loss, at the tip, of a conical section of about 0.1 mm height. The truncation obviously affects the velocity distribution within the fluid and accordingly the estimate of P_1. From the actual measurements we find that the variation of $p_{22}(r)$ is very nearly a logarithmic function of the radius (over most of the area of the plate) as suggested by (2.4). But, because of the truncation, p_{22} must necessarily be finite at $r = 0$, since the shear rate now tends to zero as we approach the centre. Thus, to estimate the error introduced by the truncation we assume that p_{22} has the following distribution:

$$\left.\begin{aligned} p_{22} &= \text{constant} \quad (0 \leqslant r \leqslant \alpha), \\ p_{22} &= a + b\ln r \quad (\alpha \leqslant r \leqslant R), \end{aligned}\right\} \tag{2.7}$$

where a and b may be related to P_1 and P_2 by means of (2.5) and (2.4), if we further assume that the truncation does not influence the values of a and b. This assumption seems to be justified by the results of § 6.

The experimental results suggest that, if we choose α to be equal to the radius of the 'flat' on the cone, (2.7) will probably lead to a conservative estimate of the error in the total force measurement. To find the thrust F acting on the plate, p_{22} is integrated over the area of the plate and we find that

$$\frac{F_0 - F}{F_0} = \left(\frac{\alpha}{R}\right)^2 \left(1 + \frac{2P_2}{P_1}\right), \tag{2.8}$$

where F_0 is the force acting when $\alpha = 0$. In the present set of experiments it appears that $P_2 \ll P_1$

and hence the error in the estimate of F_0 is nearly equal to $(\alpha/R)^2$. For the values of α used in the course of the measurements, the quantity $(\alpha/R)^2$ is always less than 0.002, and the actual error is probably much smaller. This source of error results in a low estimate of P_1.)

Since the material functions are independent of the radius in the cone-and-plate viscometer, it follows immediately that the torque T required to rotate the cone is

$$T = \tfrac{2}{3}\pi R^3 p_{21}(\dot{s}). \tag{2.9}$$

(*c*) *The general configuration*

We now consider the more general situation depicted in figure 1 in which c is not restricted as above. In this case the normal force F acting on the annular section of the plate between the radii R_i and R may be derived easily from (2.1) and is given by (cf. Marsh & Pearson 1968)

$$F = -\pi \int_{R_i}^{R} \left\{ 2rP_2 - (r^2 - R_i^2)\left[\frac{\tan\beta}{c + r\tan\beta} P_2 + \frac{1}{r}(P_1 + P_2) \right] \right\} \mathrm{d}r. \tag{2.10}$$

If we now differentiate (2.10) with respect to c, and set c equal to zero we find that

$$\frac{\tan\beta}{\pi(R - R_i)} \left(\frac{\partial F}{\partial c} \right)_{c=0} = -\left(1 - \frac{R_i}{R}\right) \dot{s} \frac{\mathrm{d}P_1}{\mathrm{d}\dot{s}} - P_2 \left(1 - \frac{R_i}{R}\right) + 2\frac{R_i}{R} \dot{s} \frac{\mathrm{d}P_2}{\mathrm{d}\dot{s}}. \tag{2.11}$$

For the special case in which $R_i = 0$, (2.11) becomes

$$-\frac{\tan\beta}{\pi R} \left(\frac{\partial F}{\partial c} \right)_{c=0} - \dot{s} \frac{\mathrm{d}P_1}{\mathrm{d}\dot{s}} = P_2(\dot{s}), \tag{2.12}$$

a result which was first derived by Jackson & Kaye (1966). Thus if $P_1(\dot{s})$ is known we are able to estimate $P_2(\dot{s})$ from (2.12) by measuring $(\partial F/\partial c)_{c=0}$. An approximate estimate of $P_2(\dot{s})$ may also be found from (2.11), for small values of R_i/R, by neglecting the term $2(R_i/R)\,(\mathrm{d}P_2/\mathrm{d}\ln\dot{s})$; a better estimate of P_2 could then be obtained by using the first approximation to give an estimate of this neglected term.

A similar expression to that of (2.12) may be derived for any value of c. To do this we put $R_i = 0$ in (2.10) and change the variable of integration to $\dot{s}$ by means of (2.3). Carrying this out we find that

$$F/(\pi\Omega c^2) = \int_0^{\dot{s}(R)} \frac{\dot{s}\Omega(P_1 - P_2) - \dot{s}^2 \tan\beta P_2}{\Omega(\Omega - \dot{s}\tan\beta)^3} \mathrm{d}\dot{s}. \tag{2.13}$$

Now, on differentiating (2.13) with respect to c we obtain

$$P_2(\dot{s}(R)) = \left(1 + \frac{R\tan\beta}{c}\right) \left[P_1(\dot{s}(R)) - \frac{F}{\pi R^2}(2 + m) \right], \tag{2.14}$$

where $m = -\partial \ln F/\partial \ln c$. This result was first given by Marsh & Pearson (1968) and, if P_1 is known, it provides another means of measuring $P_2(\dot{s})$.

2.2. *Torsional flow between parallel plates*

This viscometer has the same arrangement as that shown in figure 1 when the cone angle β is zero. Accordingly the comments made in § 2.1 (*a*) are applicable here, but it should be noted that, in the slow-flow approximation, the equations of motion are satisfied identically (with the exception that the boundary conditions at the liquid/air interface may not be satisfied).

When $\tan\beta = 0$ we see from (2.3) that $\dot{s}\partial/\partial\dot{s} = r\partial/\partial r$, and hence from (2.1) the radial distribution of the normal stress p_{22} is given by

$$r\frac{\partial p_{22}}{\partial r} = P_1 + P_2 + \dot{s}\frac{\mathrm{d}P_2}{\mathrm{d}\dot{s}}. \tag{2.15}$$

PHILOSOPHICAL TRANSACTIONS OF THE ROYAL SOCIETY A MATHEMATICAL, PHYSICAL & ENGINEERING SCIENCES

If we now integrate (2.15) we find that

$$p_{22}(\dot{s}) - p_{22}(0) = P_2(\dot{s}) + \int_0^{\dot{s}} (P_1(\zeta) + P_2(\zeta))\, \zeta^{-1}\, \mathrm{d}\zeta. \tag{2.16}$$

The total normal force acting on the plates may be found from (2.13) by putting $\tan\beta = 0$, and with the aid of (2.3) is given by

$$F = \frac{\pi R^2}{(\dot{s}(R))^2} \int_0^{\dot{s}(R)} (P_1(\dot{s}) - P_2(\dot{s}))\, \dot{s}\, \mathrm{d}\dot{s}. \tag{2.17}$$

On differentiating (2.17) with respect to $\dot{s}(R)$ we deduce the result of Kotaka, Kurata & Tamura (1959):

$$P_1(\dot{s}(R)) - \frac{2F}{\pi R^2} - \frac{\dot{s}(R)}{\pi R^2} \frac{\partial F}{\partial \dot{s}(R)} = P_2(\dot{s}(R)). \tag{2.18}$$

Thus, knowing $P_1(\dot{s})$, we may determine $P_2(\dot{s})$ from measurements of $F(\dot{s}(R))$.

2.3. *Flow between concentric cylinders*

In this viscometer a Couette flow is generated between a pair of concentric cylinders by rotating one of the cylinders with a steady angular velocity Ω, keeping the other cylinder fixed. The paths of individual fluid elements are assumed to be circular and to be concentric with the two cylinders, as a result of which both the equations of motion and the boundary conditions are satisfied exactly for the case of extremely long cylinders. However, in the laboratory there will be regions near the (axial) extremities of the fluid where these conditions are not satisfied, thereby giving rise to secondary flows, the importance of which must be investigated experimentally.

By considering the stress distribution on a small element of fluid, between adjacent streamlines of the flow, it is easily shown (cf. Lodge 1964, pp. 190–192) that, for equilibrium in the radial direction,† we must have

$$r\partial p_{22}/\partial r = P_1(\dot{s}), \tag{2.19}$$

where r is the radius of curvature of the streamline under consideration. From the stress distribution in the tangential direction we see that

$$r\partial p_{21}/\partial r = -2p_{21}(\dot{s}). \tag{2.20}$$

The local shear rate is determined by the angular velocity distribution $\omega(r)$ and is (see Lodge 1964, pp. 344–346)

$$\dot{s} = r\, \mathrm{d}\omega/\mathrm{d}r. \tag{2.21}$$

Then by integrating (2.19) across the gap between the cylinders it follows from these results that

$$\Delta p_{22} = \frac{1}{2} \int_{\sigma_i - \delta}^{\sigma_i} P_1(\sigma)\, \mathrm{d}\sigma, \tag{2.22}$$

where Δp_{22} is the difference between p_{22} acting at the outer and inner cylinders respectively; σ denotes $\ln|p_{21}|$, and has the value σ_i at the inner cylinder. From (2.20) we see that the value of σ at the outer cylinder may be expressed in terms of σ_i and the ratio κ of the radii of the inner and outer cylinders; for convenience we write $\delta = -2\ln\kappa (= 2\ln(R_0/R_i))$.

For a given fluid the velocity distribution $r\omega(r)$ is determined by the angular velocity Ω of the moving cylinder. When the inner cylinder rotates it follows from (2.20) and (2.21) that

$$\Omega = \frac{1}{2} \int_{\sigma_i - \delta}^{\sigma_i} \dot{s}(\sigma)\, \mathrm{d}\sigma. \tag{2.23}$$

† In deriving (2.19) it is assumed that no body forces act within the fluid. However, in practice, the centrifugal force field gives rise to an additional, unwanted, gradient of p_{22} which must be subtracted from the measurements. But this correction is easily accounted for; it is discussed further in § 3.

PHILOSOPHICAL TRANSACTIONS OF THE ROYAL SOCIETY A MATHEMATICAL, PHYSICAL & ENGINEERING SCIENCES

Thus if the material function $p_{21}(\dot{s})$ is known we are able to determine σ_i and hence the shear rates at the inner and outer cylinder walls for a given value of Ω. We note that (2.23) depends upon the material function $p_{21}(\dot{s})$ and so, for a given speed of rotation, the velocity distribution differs according to the material: Pipkin (1968) has chosen to call flows of this kind 'partially controllable' to distinguish them from flows of the kind discussed in §§ 2.1 and 2.2 in which the shear rate at a given fluid element is independent of the material properties.

We are now in a position to determine $P_1(\sigma)$ from the relations (2.22) and (2.23) by making measurements of Δp_{22} and Ω (and knowing $p_{21}(\dot{s})$). To invert (2.22) to find $P_1(\sigma_i)$ we follow the method suggested by Coleman *et al.* (1966): from (2.22) we have

$$P_1(\sigma_i) - P_1(\sigma_i - \delta) = 2\left(\frac{\partial(\Delta p_{22})}{\partial\sigma}\right)_{\sigma_i}, \tag{2.24}$$

and by determining empirically the quantity $\partial(\Delta p_{22})/\partial\sigma$ at $\sigma = \sigma_i - n\delta$ $(n = 0, 1, 2, \ldots)$ we find, on summing terms, that

$$P_1(\sigma_i) = 2\sum_{n=0}^{\infty}\left(\frac{\partial(\Delta p_{22})}{\partial\sigma}\right)_{\sigma_i - n\delta}. \tag{2.25}$$

When the ratio, κ, of the cylinder radii is not too near one the series (2.25) converges fairly rapidly, and in the current measurements only three or four terms of the summation were required.

2.4. *Stress-optical methods*

In order to provide as many independent checks as possible we have used stress-optical measurements to give an additional estimate of P_1. These methods have been used fairly widely and with remarkable success (a recent survey article by Janeschitz-Kriegl (1969) discusses many of the results). In particular Kaye *et al.* (1968) found extremely good agreement between their stress-optical measurements on the one hand and their mechanical measurements on the other.

In general a molecule becomes polarized in the presence of light, so that an aggregation of molecules, forming say a liquid or a gaseous phase, may exhibit optical-birefringence properties. In solutions of long-chain polymer molecules this effect is pronounced and the birefringence may readily be measured: for such solutions (at a given temperature) we shall assume that the refractive-index tensor $\boldsymbol{n}$ may be related to the stress tensor $\boldsymbol{p}$ thus:

$$\boldsymbol{n} = C\boldsymbol{p} + A\boldsymbol{1}, \tag{2.26}$$

where C and A are scalar quantities. Although (2.26) is taken as an assumption, this kind of relation is not unexpected on the basis of molecular theories: for a permanent network of long-chain molecules a relation of the form (2.26) has been derived (see Lodge 1960) when the configuration of states of equal potential energy is a Gaussian distribution, an approximation that is expected to be valid for extremely long polymer chains. Lodge (1960) suggests how the theory may be relaxed to apply to a liquid for which no *permanent* network exists, but for which a temporary network may be defined such that a molecule passes through almost all its configurational states before the network undergoes a change. The theory accordingly predicts that the stress-optical coefficient C is independent of the rate of shear, of the concentration of the solution, and of the distribution of molecular weights of the molecules.

For a shear flow $(v^1(x^2), 0, 0)$ it is usual to make optical measurements of Δn, the difference between the *principal* refractive indices of $\boldsymbol{n}$ in the 1-2 plane, and of χ', the inclination of the principal direction in the 1-2 plane to the 1-direction. If Δp and χ denote the corresponding

quantities for the stress tensor $\boldsymbol{p}$, it follows from (2.26) that

$$\left.\begin{aligned}\Delta n &= C\Delta p\\ \text{and}\qquad \chi' &= \chi.\end{aligned}\right\} \tag{2.27}$$

But from the well-known relations describing the principal axes of the stress tensor (see, for example, Lodge 1964, p. 66) it follows from (2.27) that

$$(\Delta n \sin 2\chi')/2p_{21} = C, \tag{2.28a}$$

and

$$2p_{21}\cot 2\chi' = P_1. \tag{2.28b}$$

Thus, by measuring Δn, χ' and p_{21} we are able to estimate P_1 and to run an independent check on the constancy of the stress-optical coefficient C. Very impressive experimental verification of (2.28*a*) has been demonstrated by a number of workers (see Janeschitz-Kriegl 1969): for example Philippoff (1964) finds a constant value for C, in a set of measurements, at values of the shear rate covering a range of more than three decades.

Thus, although the predictions of the stress-optical theory are not known to be corollaries of the simple-fluid assumptions, the method itself is of undoubted value as an experimental aid. We shall use it to provide an additional independent check on the estimate of the primary normal-stress difference, P_1.

3. Experimental apparatus

All pieces of apparatus used in this project have hitherto been described in detail in the literature, or are commercially produced machines, and thus we shall discuss here only the salient features of each machine. A summary of the measurements made on each piece of apparatus is given in table 1 at the end of this section. In some cases the same kind of measurements have been made on more than one machine in an attempt to compare the reliability of each instrument. Thus, briefly, the following instruments were used:

(I) The apparatus of Adams & Jackson (1967) for the measurement of torques and normal forces. This apparatus consists of a rotating upper member and a lower plate suspended from three fine wires. The suspension is arranged so that forces normal to the plate are converted to an angular displacement of the plate and hence may be balanced by an externally applied torque; dependent upon the sense of rotation, this 'effective torque' either adds to, or subtracts from, the torque arising from the shear stresses in the liquid. In operating the machine a carefully adjusted external torque is applied to the lower plate so that *no net displacement* of the plate occurs. By measuring this torque, for both senses of rotation of the upper member, we can deduce the normal thrust and the torque acting on the plate. This null-displacement technique ensures that there is no change in the separation between the two platens as a result of the forces acting within the liquid.

The free surface of the liquid at the edge of the apparatus was of the form indicated in figure 1*a*. Thus it is important that the shape of the free surface does not change by a significant amount when the platen is rotated, or else the surface-tension forces may lead to significant errors. From visual observations of the free surface this assumption seems to be well borne out at low shear rates. At the higher shear rates, however, changes in the shape of the free surface were noticeable, but the changes were such that the resulting error was expected to be very small in relation to the forces being measured. On the other hand, the presence of the free surface necessarily gives rise to secondary flows in the liquid, as suggested in § 2.1, and the effects of these are not easily

determined with the present machine. But there is some evidence that the influence of these secondary flows is small, since from the measurements of the normal force between parallel plates, it is observed (see § 9.3 below) that the measured force is independent of the gap between the plates and depends only on the shear rate at the rim, as indicated by (2.17): when the gap between the plates is changed the angular velocity of the rotating member must be altered to maintain the same rate of shear at the rim, and this presumably would affect the nature of the secondary flows, yet no significant changes in the thrust were observed.

There are other possible sources of error in these measurements, and these are discussed below in connexion with apparatus IV.

The main dimensions of the apparatus are: the platen radius, $R = 4.98$ cm; the cone angle $\beta = 3.10°$.

(II) A Weissenberg rheogoniometer (model R 16) at Madison. This machine is used to make basically the same measurements as the previous machine, though the actual method of measurement is a little different. The torque is determined from the (small) twist of a torsion rod; the normal forces are found from the (small) deflexion of a leaf spring on which rests one of the platens. The spring is rigidly clamped at one end and at the other rests on a support: the support is raised by a servo system, according to the deflexion of the spring, so that the gap between the platens is held constant. The liquid boundary at the rim is of the same form as that used in apparatus I (and sketched in figure 1*a*). Hence the remarks made about I, regarding possible errors in estimates of P_1 made on the basis of the normal-thrust measurements, apply to this apparatus as well.

The platens used with this machine had radii of 3.75 cm; the cone angle was 1.00°.

All measurements with this instrument were made by Dr E. K. Harris, Jr. of the Chemical Engineering Department at Madison.

(III) A Weissenberg rheogoniometer (model R 16) at Manchester. The comments about apparatus II apply also to this machine. The measurements in this case were made by a laboratory technician.

The platens used for these measurements had radii of 5.00 cm; the cone angle β was 1.08°.

(IV) The apparatus of Adams & Lodge (1964) for measuring the normal-stress distribution. This machine consists of a rotating upper member and a lower plate in the form of a tray. Drilled into the lower plate are three small (0.122 mm diam.) holes leading to a large cavity at the bottom of which is a thin metal diaphragm (the arrangement is illustrated schematically in figure A 1 of the appendix). When the working fluid fills the cavity the diaphragm may be used as a pressure transducer by applying a static pressure to the side opposite the working fluid so that there is no net displacement of the diaphragm. The value of the applied static pressure is then used to estimate the normal stress acting on the surface of the plate near the hole. The lower plate may be moved in a direction normal to the axis of rotation with the result that measurements may be made at any desired radius. The free surface of the liquid may take either of the configurations sketched in figure 1.

A large number of potentially important sources of error have had to be considered in the design of this apparatus: for example, too large a misalinement of the axis of the rotating member with the normal to the stationary plate may give rise to non-negligible errors (see Adams & Lodge 1964). Another source of error discussed by Adams & Lodge arises from the axial movement of the rotating member: because of the high viscosities of the fluids usually employed, Adams & Lodge advise that the axial displacement of this member should be less than about 0.05 μm to

reduce the error to negligible proportions. Similar considerations were taken into account in the design of apparatus I.

The following platens were used with this machine: cones of radii 4.41 cm and β-angles of 5.67°, 3.266°, 1.718°; a cone of radius 6.03 cm and β-angle 3.267°; a flat plate of radius 4.41 cm.

(V) The flow-birefringence apparatus of Kaye & Saunders (1964). This instrument consists of a pair of concentric cylinders, the outer of which may be rotated at a steady speed about the common axis. The difference in radii between the two cylinders is much less than the individual cylinder radii so that the rate of shear is nearly uniform across the annular gap containing the working fluid. The shear stress in the liquid may be determined by measuring the torque exerted on the inner cylinder. The optical birefringence and extinction angle may be determined by shining a narrow beam of plane-polarized light parallel to the common axis of the cylinders and through the liquid gap: the extinction positions and total phase retardation are observed for the emergent, elliptically polarized, light.

The radius of the inner cylinder is 6.75 cm and the width of the annular gap is 0.193 cm. The path length of the light beam through the test liquid is about 22 cm.

All measurements with this apparatus were made by Dr A. Kaye.

(VI) The concentric cylinders of Broadbent & Lodge (1971) in which the normal stress p_{22}, acting on the cylinder walls, may be measured. The machine consists of a pair of concentric cylinders of which the inner cylinder is rotated at a steady speed. The normal stresses acting on the walls of the inner and outer cylinders are measured by means of transducers of the kind used with apparatus IV (and see appendix A). The radii of the inner and outer cylinders could be changed by the insertion of cylindrical sleeves. The following sizes were available:

inner cylinder radii, $R_i = 6.480\,\text{cm};\ 8.303\,\text{cm};$

outer cylinder radii, $R_o = 9.771\,\text{cm};\ 11.862\,\text{cm}.$

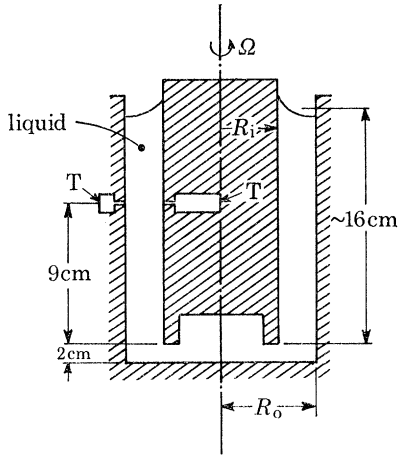

FIGURE 2. A schematic drawing of the concentric cylinders of Broadbent & Lodge (1971). T denotes the stress-measuring transducers.

The disposition of the cylinders is shown schematically in figure 2. To obtain meaningful data from this apparatus there must be extensive regions above and below the measuring transducers where the velocity field closely approximates to that hypothesized in § 2.3 (namely that all fluid particles move in circles concentric with the cylinders). Deviations from this flow necessarily arise at the upper and lower boundaries of the apparatus: the upper surface of the liquid is free

and should not be an important source of generation of secondary flows (but large distortions of the free surface, because of the Weissenberg effect, may negate this assertion); the lower end of the cylinder is some distance from the bottom of the container (see figure 2) to help reduce the effect of secondary flows generated at the lower fixed boundary. Broadbent & Lodge have indirectly investigated the influence of these effects by making a series of measurements in which the depth of the liquid and the position of the measuring transducer, relative to both the upper and lower boundaries, was varied. From their measurements Broadbent & Lodge suggest that the secondary flows are of negligible importance. We shall make the same assumption with regard to the current measurements.

The largest value of the Reynolds number $R_i \Omega^2/\nu$ for these experiments, was about 1.3. ν is the kinematic viscosity.

There is also the possibility that the flow deviates from the postulated motion as a result of the Taylor instability of Couette flow. For viscous Newtonian fluids the critical operating conditions beyond which the instability is manifested have been carefully investigated both theoretically and experimentally (see Chandrasekhar 1961). Thus when the inner cylinder rotates and the outer cylinder is held fixed, the instability occurs when the Taylor number $Ta(=\frac{64}{9}(\Omega R_i^2/\nu)^2)$ exceeds 3.31×10^4, for the case in which $R_i/R_o = 0.5$. However, the circumferential velocity distribution, for a fluid whose viscosity depends upon the shear rate, differs greatly from that of a Newtonian fluid and hence it is to be expected that the critical Taylor numbers also differ by a wide margin. Because of the far larger radial gradient of the circulation usually encountered near the inner cylinder in the non-Newtonian case, it is expected that the critical Taylor number will be considerably less than that for Newtonian fluids. Thomas & Walters (1964*a*, *b*) have shown that the presence of elasticity in the fluid can considerably lower the value of the critical Taylor number at which instability occurs. In the present experiments we are unable to say that instability did not occur and if it did we must assume that it had negligible influence on the results. Two pieces of evidence support this: first, the largest Taylor number occurring in the experiments (based on the smallest observed value of ν, and on the largest Ω employed) was about 10, and usually it was much smaller than this; thus any secondary flows are likely to have been weak. Secondly, there were no observed fluctuations or anomalous results noticed during the course of the experiment.

When we interpret the results of measurements taken with this apparatus corrections must be made for unwanted stresses arising from centrifugal forces in the fluid. The fluid in the cavity of the inner cylinder rotates essentially as a rigid body and thus contributes to the stress acting on the transducer diaphragm at the bottom of the cavity. Since the axis of rotation passes through the centre of the diaphragm, it follows that the magnitude of this correction (p_u) is $\frac{1}{2}\rho R_i^2 \Omega^2$, where ρ is the density of the liquid. Also, a correction must be applied for the contribution to the stresses arising from the centrifugal forces of the rotating liquid in the annular gap (see Coleman *et al.* 1966). This correction has a magnitude p_c, where

$$p_c = \int_R^{R_o} \rho r \omega(r)^2 \, \mathrm{d}r. \tag{3.1}$$

$\omega(r)$ is the angular velocity of the fluid at the radius r, and is given by an integral of the form (2.23). Integral (2.23) is dependent upon the material function $p_{21}(\dot{s})$ and therefore it must, in general, be evaluated graphically. However, it appears that the function

$$\dot{s} = \mathscr{A} p_{21}^{\mathscr{B}}, \tag{3.2}$$

where $\mathscr{A}$, $\mathscr{B}$ are constants, is a good approximation to the experimental data (cf. § 8.3). Thus the

use of (3.2) to evaluate (3.1) should yield a good approximation to p_c. Using the relation (3.2) and an integral of the form (2.23) we find, in the case of a stationary outer cylinder, that

$$\omega = \frac{\dot{s}_i \kappa^{2\mathscr{B}}}{2\mathscr{B}} \left\{ \left(\frac{R_o}{r} \right)^{2\mathscr{B}} - 1 \right\}, \tag{3.3}$$

where $\dot{s}_i$ is the shear rate at the inner cylinder. It now follows from (3.1) that

$$p_c = \rho R_i^2 \Omega^2 \frac{\kappa^{4\mathscr{B}-2}}{1-\kappa^{2\mathscr{B}}} \left(\frac{1-\kappa^{2-4\mathscr{B}}}{2-4\mathscr{B}} - \frac{1-\kappa^{2-2\mathscr{B}}}{1-\mathscr{B}} + \frac{1-\kappa^2}{2} \right). \tag{3.4}$$

The correction for a Newtonian fluid is found by putting $\mathscr{B} = 0$ in this expression. But for Newtonian fluids $P_1 \equiv 0$, and hence, from (2.22), it follows that non-zero measurements of Δp_{22} arise entirely from these centrifugal contributions. Broadbent & Lodge (1971) have made a careful check of this result, and their measurements are in good agreement with the prediction; moreover, their measurements of the stresses acting on the individual walls of the cylinders also accord extremely well with the theoretical values for a Newtonian fluid.

In the present experiments $\mathscr{B} \approx 2.7$ and it happens that the total correction $p_u + p_c$ is nearly the same as that for the Newtonian fluid, but we shall use (3.4) to calculate p_c.

In table 1 a summary is given of the measurements made on each instrument and the quantities which may be deduced from these measurements.

TABLE 1. SUMMARY OF THE EXPERIMENTAL MEASUREMENTS AND OF THE DERIVED QUANTITIES

The code for the instruments is: (I) Adams & Jackson (1967); (II) Weissenberg, rheogoniometer at Madison; (III) Weissenberg rheogoniometer at Manchester; (IV) Adams & Lodge (1964); (V) Kaye & Saunders (1964); (VI) Broadbent & Lodge (1971).

viscometer	instrument used	measured quantity	derived quantity	reference equation
cone and plate ($c = 0$)	I, II, III	normal force F	P_1	(2.6)
	I, II, III	torque T	p_{21}	(2.9)
	IV	normal stress distribution $r\partial p_{22}/\partial r$	$P_1 + 2P_2$	(2.4)
	IV	normal stress at the rim $p_{22}(R)$	P_2	(2.5)
cone and plate (general values of c)	I, II	normal force $F(c)$	P_2	(2.12), (2.14)
	IV	normal stress p_{22} integrated over an annulus of the plate to give $F(c)$	$P_2 + O\left(\frac{dP_2}{d\ln \dot{s}}\right)$	(2.11)
plate and plate	I, II	normal force $F(\dot{s})$	P_2	(2.18)
	IV	normal-stress distribution		
		(a) $r\partial p_{22}/\partial r$	$P_1 + P_2 + \frac{dP_2}{d\ln \dot{s}}$	(2.15)
		(b) $p_{22}(\dot{s}) - p_{22}(0)$	$P_2 + \int_0^{\dot{s}} (P_1 + P_2)\,\zeta^{-1} d\zeta$	(2.16)
concentric cylinders	V	torque	p_{21}	
	V	birefringence extinction angle χ'	P_1	(2.28)
	VI	normal stress on the cylinder walls Δp_{22}	P_1	(2.22), (2.25)

4. PREPARATION AND STABILITY OF THE LIQUID

4.1. *Preparation*

The liquid used for the experiments was a solution of a high molecular mass polyisobutene, 'oppanol B200' ($M_w = 4.5 \times 10^6$, $M_w/M_n = 2.0$), in a low molecular mass polyisobutene, 'oppanol B1' ($M_w = 400$; viscosity at 25 °C = 0.25 P). A quantity of the B200, weighing 150 g, together with 6 l of hexane was placed in a 20 l flask which was then rotated slowly about an axis inclined to the vertical. After 13 days of mixing the solution appeared, to the eye, to be homogeneous and a quantity of the liquid polymer B1 was added to the flask. The flask was now

rotated for a further 23 days, by which time the solution again appeared to be homogeneous. The hexane was then removed by means of a vacuum pump with a stream of nitrogen passing through the solution to aid nucleation. The pumping was continued for a total period of 58 h, the last 10 of which yielded negligible quantities of hexane. The solution was then decanted to smaller containers, sealed, and stored at 4 °C. The components of the solution were added in the proportion of 3.05 g of B 200 per 100 g of B 1 (or in equivalent terms 24.8 g of B 200 per litre of B 1).

A small part of the solution (kept at 4 °C) was flown to Madison to be tested there.

4.2. *Stability*

A technique to characterize the stability of the physical properties of a solution, as a function of time, has been suggested by Lipson & Lodge (1968). This characterization uses the extremely accurate measurements of the quantity $r(\partial p_{22}/\partial r)$ obtainable with apparatus IV: for the cone-and-plate apparatus this quantity is a constant and the experimental results show that p_{22} varies logarithmically with the radius to within a standard deviation of about 0.5 % of $r(\partial p_{22}/\partial r)$. Thus Lipson & Lodge (1968) suggest that their polyisobutene solution retained, at 25 °C, the same physical properties for a period of about 8 days, after which the liquid properties began to change, probably as a result of chemical oxidation of the long-chain molecules. Using the same test Pritchard (1970) found that a similar polyisobutene solution exhibits no measurable changes over a period of at least 140 days, if it is kept in a sealed flask at a temperature of 4 °C. Following a similar procedure with the present solution it has been found that the physical properties are preserved for at least 9 months. However, when the liquid is removed from storage and placed in one of the measuring instruments, at room temperature,† it is essential to know the period of time during which reliable data may be taken. Accordingly, apparatus IV was filled with the solution and the gradient $r(\partial p_{22}/\partial r)$ measured at various times over a period of 51 days. (Actually we shall denote the quantity determined in the measurement by $r(\partial \bar{p}/\partial r)$, where $\bar{p}$ represents the mean value of the pressure observed (cf. appendix A) in the clockwise and anticlockwise directions.)

This experiment was carried out with a 'sea of liquid' surrounding the cone (as shown in figure 1*b*) so that the plate could be moved in a direction normal to the axis: only two positions of the plate are needed to yield six measurements of $\bar{p}(r)$ which is usually sufficient information to define $r(\partial \bar{p}/\partial r)$ fairly accurately. The values of $r(\partial \bar{p}/\partial r)$ determined in this way are indicated by the open circles in figure 3. After a certain time the value of $r(\partial \bar{p}/\partial r)$ deviates from that measured in the early stages of the experiment; also the standard deviation of each result increases with the day number of the experiment. From the distribution $\bar{p}(\ln r)$ obtained at each measurement it appears that the increased variance arises from the two determinations of $\bar{p}$ nearest the rim of the cone, and lying within a radial distance from the rim of about the same magnitude as the lateral movement of the plate. Thus it appears that the liquid in the 'sea' beyond the rim of the cone is oxidized at a rate different from that near the axis of the cone, with the result that the solution is probably no longer homogeneous. On the other hand, the four measurements of $\bar{p}$ nearest the axis of the cone may be used to define $r(\partial \bar{p}/\partial r)$ over a region in which the fluid appears to be more homogeneous. The result of recalculating $r(\partial \bar{p}/\partial r)$ in this way is also shown in figure 3 (filled circles): in this case the magnitude of $r(\partial \bar{p}/\partial r)$ decreases with time, except for the initial period of 10 to 12 days, but its standard deviation is nearly the same at each determination.

† All measurements in this paper were made at 25.0 °C.

Since $r(\partial p_{22}/\partial r)$, and hence the related quantity $r(\partial \bar{p}/\partial r)$, is a measure of $P_1 + 2P_2$ (see (2.4)), it would appear from these results that the physical properties of the solution change with time, probably because of degradation of the polymer molecules. However, the results suggest that fairly reliable data may be taken for a period of up to 10 days before the physical properties undergo significant changes.

A similar test was also carried out for degradation under prolonged shearing, and, after a total of 30 h shearing of the liquid, no significant changes in the material properties were observed.

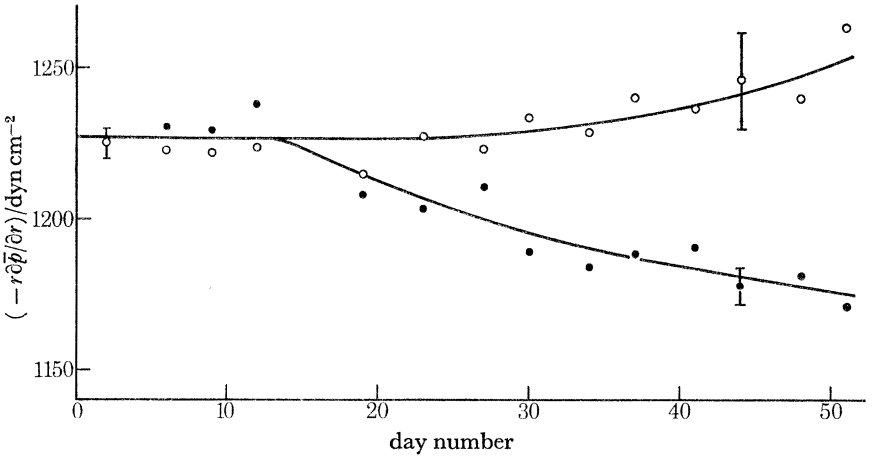

FIGURE 3. A test of the constancy of the physical properties of the liquid as a function of time. The test was made in apparatus IV at 25 °C; the shear rate $\dot{s} = 1.74\,\mathrm{s}^{-1}$; the cone angle $\beta = 3.27°$. The quantity plotted is $-r\partial\bar{p}/\partial r$: ○, from all the data; ●, only the data near the axis of rotation. (1 dyn = 10^{-5} N.)

5. MEASUREMENTS OF THE SHEAR-STRESS FUNCTION

The shear-stress function p_{21} was measured, following the methods outlined above, on instruments I, II, III and V. The measurements of $p_{21}(\dot{s})$ obtained from instruments I and V are shown in figure 4. As a rough guide, it is anticipated that these measurements will be accurate to within about 2 to 3 % in the case of the concentric cylinders (apparatus V), and to within about 5 % with the cone-and-plate viscometer of Adams & Jackson (apparatus I). It follows from the graph that all the measurements of p_{21} lie well within a 5 %-band (indicated by the bar on the curve) of the approximate 'curve of best fit'. (In drawing this curve slightly more weight has been given to the measurements from apparatus V.) Thus, we shall assume henceforth that the curve of figure 4 represents the shear-stress function over the range of shear rates covered by the measurements. Also shown in figure 4 is the viscosity η, defined by the relation $\eta = p_{21}/\dot{s}$, which is seen to change by an order of magnitude over the range of shear rates covered by the measurements.

Some molecular theories (see, for example, Zimm 1956) predict, for sufficiently low shear rates, that the viscosity is independent of the shear rate. Indeed a theorem of Coleman & Noll (1960) shows that *all* simple fluids behave as second-order fluids, at sufficiently low shear rates, and have a viscosity that is essentially constant. Accordingly, the abscissa of figure 4 has also been scaled in terms of a dimensionless shear stress $\tilde{p}_{21} = p_{21}/nkT_0$ suggested by these molecular theories (cf. Janeschitz-Kriegl 1969), where n is the number of long chain molecules per unit volume, k is Boltzmann's constant, and T_0 is the absolute temperature. We expect that the second-order-fluid approximation is realized only for values of $\tilde{p}_{21} \ll 1$; these conditions were not attained in the present experiments.

The measurements of $p_{21}(\dot{s})$ made with instruments II and III are shown in figure 5 and the results are compared with the curve of figure 4. Since Harris (1970) suggests that apparatus II cannot be expected to be reliable to within $\pm 5\,\%$, the results of figure 5 may be deemed to agree, to within the measuring error, with the measurements shown in figure 4.

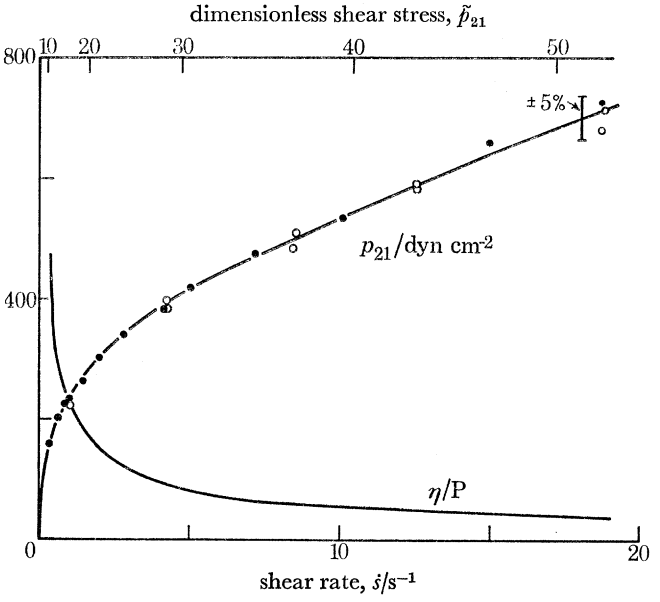

FIGURE 4. The shear-stress function $p_{21}(\dot{s})$. ○, Cone-and-plate measurements made with apparatus I, $\beta = 3.27°$; ●, measurements from concentric cylinders, apparatus V. ——, Approximate mean representation of the data. ($1\,\mathrm{P} = 10^{-1}\,\mathrm{Pa\,s}$.)

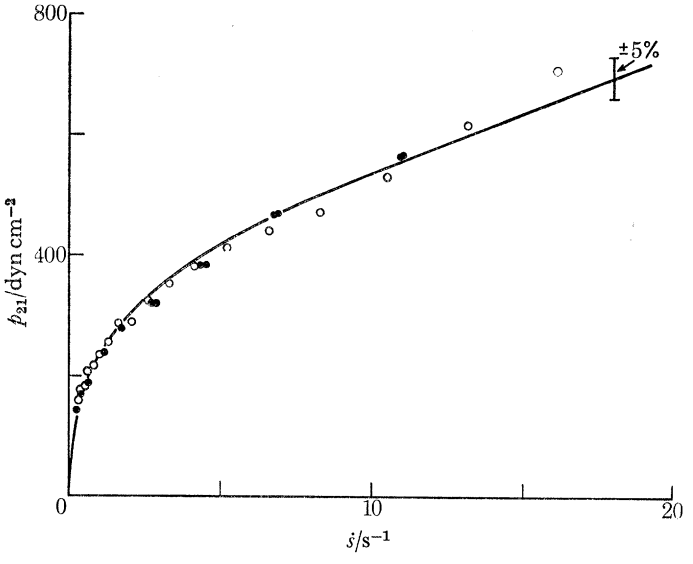

FIGURE 5. A comparison of the shear-stress function of figure 4 with other measurements: ●, cone and plate (apparatus II) at Madison, $\beta = 1.00°$; ○, cone and plate (apparatus III) at Manchester, $\beta = 1.08°$.

Thus, consistent measurements of the shear-stress function have been obtained from four instruments, each differing from the others in some feature. So it would appear, as far as the shear stress is concerned, that the possible sources of error mentioned above are of negligible importance in these experiments.

6. The primary normal-stress difference

Using the three methods for measuring the primary normal-stress difference indicated in table 1, P_1 has been measured on a total of five instruments. The results of the measurements made at Manchester with instruments I, V and VI are shown in figure 6; but, alas, no two of the sets of data are in agreement over the entire range of the measurements. However, for shear rates below $6\,s^{-1}$ the results from the cone-and-plate apparatus (I) and the optical measurements,

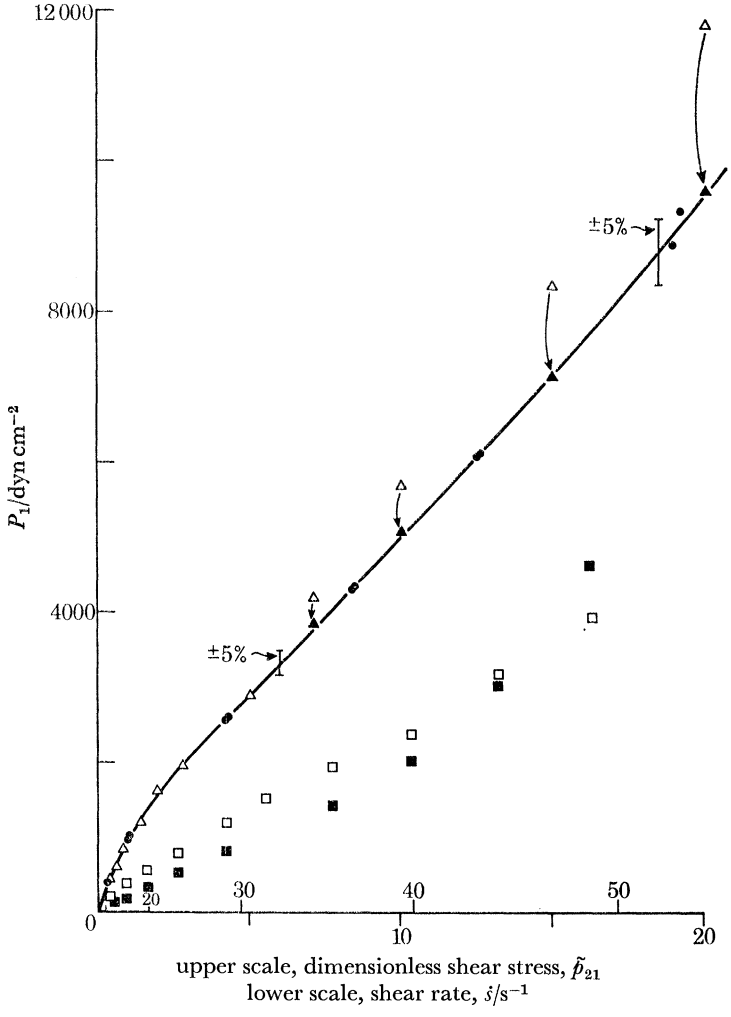

Figure 6. The normal-stress difference $P_1(\dot{s})$. ●, Cone-and-plate measurement with apparatus I, $\beta = 3.27°$. △, Stress-optical measurement, apparatus V. ▲, stress-optical results after correction (see text). □, concentric cylinders, apparatus VI, $\kappa = 0.577$. ■, concentric cylinders, apparatus VI, $\kappa = 0.700$. ——, Curve assumed to represent $P_1(\dot{s})$.

indicated by open circles, are in very good agreement. The results from the concentric cylinders (apparatus VI) are not in agreement with either of the other two sets of data: indeed the measurements made with cylinders of different radii do not even agree with each other, in contradistinction to the results of Markovitz (1965*b*) who observed a close agreement between measurements taken with two different values of κ (the ratio of the radii of the inner and outer cylinders). That the measurements from the concentric cylinders would not agree with the other data was expected

because of the use of cavities in the walls of the cylinders to measure the stress p_{22}. The discussion in appendix A indicates how this measuring technique may lead to large systematic errors in determining p_{22}, and accordingly the disagreement in figure 6 is believed to be a manifestation of this phenomenon. Moreover, the error in p_{22} is expected to depend upon κ and indeed we see in figure 6 that the results for $\kappa = 0.577$ and $\kappa = 0.700$ are different. A discussion of the possible resolution of this disparity is given in § 8.3.

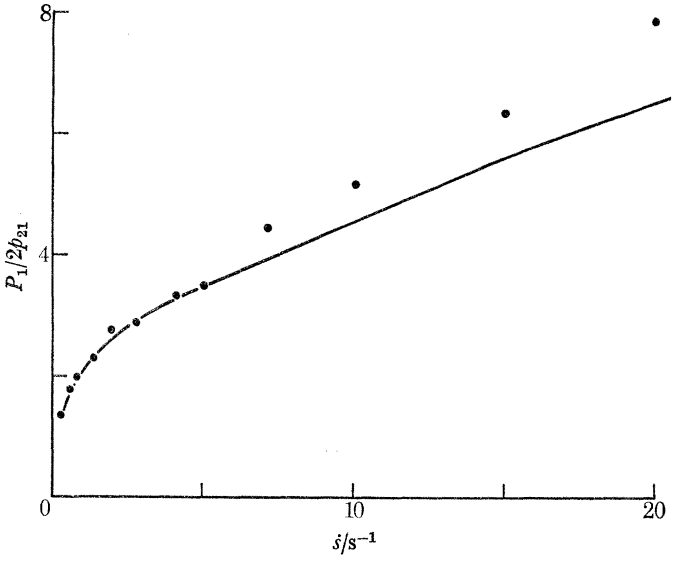

FIGURE 7. The ratio of the primary normal-stress difference to the shear stress. ——, Derived from the representations assumed in figures 4 and 6; ● are derived from optical measurements of the extinction angle χ', apparatus V.

Let us assume, for the present, that the measurements made with the cone-and-plate apparatus (the filled circles of figure 6) nearly represent the function P_1, and accordingly that the curve of figure 6 is a good approximation to $P_1(\dot{s})$ over the range of the measurements. This function has been replotted in dimensionless form in figure 7, where P_1 has been made dimensionless with respect to the shear stress. From the geometrical properties of the stress ellipsoid it follows that P_1/p_{21} is a measure of the orientation χ of one of the principal axes of the stress ellipsoid to the 1-direction of the flow (cf. (2.28*b*)). But the use of the optical measurements depends on the assumption that χ is equal to the extinction angle χ' (see (2.27)), and for this reason the measurements of χ' made on apparatus V are also shown in figure 7. For shear rates less than about $6\,s^{-1}$ the data agree well with the curve derived from figure 6, but the four measurements of χ' made at the higher shear rates deviate from the expected result. It is thought that these four optical measurements are in error, and that the difficulty is a consequence of the Weissenberg effect which causes the free surface of the liquid to rise near the inner cylinder when Couette flow is established between a pair of concentric cylinders. At the higher shear rates this effect is believed to have been large enough to expose, at least partially, the upper window through which the light beam passes, thereby interfering with the beam and introducing a small error to the extinction angle χ'. Kaye *et al.* (1968), using a less concentrated solution, did not encounter this difficulty and obtained good agreement between both measurements over the entire range of the experiment.

Fortunately it is possible to make an independent check of the optical measurements by means of (2.28*a*) since the stress-optical relation (2.26) is valid only if the stress-optical coefficient C is a constant. The value of C determined at each measurement is shown in figure 8, from which

it is evident that C is not a constant. On the other hand, C *is* constant, to within the experimental accuracy, at the lower shear rates; it has a mean value, indicated by the dashed line, of 1.66×10^{-10} cm²/dyn when the four readings at the higher shear rates are excluded. This value of C is in good agreement with the value of 1.68×10^{-10} cm²/dyn obtained by Kaye *et al.* (1968) for a 2 % solution of polyisobutene B 200 in polyisobutene B 1, and by Mr D. M. Bancroft (private communication, and see Kaye *et al.* 1968) for solutions of various concentrations of polyisobutene in decalin. As indicated in § 2.4 the theory suggests that C is independent of the rate of shear and of the concentration of the solution, and accordingly the very close agreement between all these

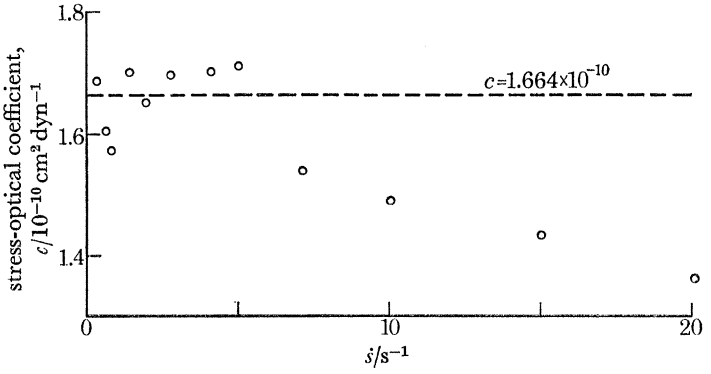

FIGURE 8. The stress-optical coefficient C measured on apparatus V. – – –, Mean value of the measurements made at the lower shear rates.

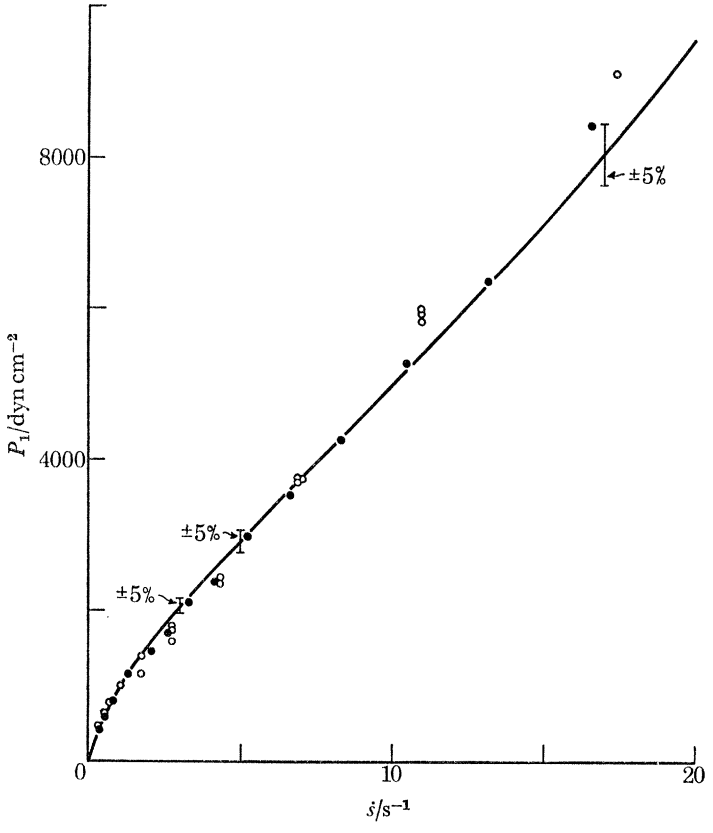

FIGURE 9. A comparison of the material function P_1 shown in figure 6 with other measurements. ○, Cone and plate (apparatus II) at Madison, $\beta = 1.00°$; ●, cone and plate (apparatus III) at Manchester, $\beta = 1.08°$.

measurements of C provides a good basis for adopting, in the present measurements, the value of the stress-optical coefficient given by the results at the lower shear rates. Thus, if we assume that $C = 1.66 \times 10^{-10}\,\mathrm{cm^2/dyn}$, and since we know the values of Δn and p_{21} at each measurement, we may recalculate χ' via (2.28).† Following this procedure we may deduce new 'optical' estimates of P_1, the results of which are indicated by the dark triangles of figure 6. The agreement of these new estimates of P_1 with the data from the cone-and-plate apparatus is extremely close, indeed so close that we feel justified in taking the curve of figure 6 to be a good approximation to $P_1(\dot{s})$.

The results of the two measurements of P_1 made on the Weissenberg rheogoniometers at Madison and at Manchester are shown in figure 9 where they are compared with the curve representing the data of figure 6. The measurements from the instrument at Manchester are, in the main, in good agreement with the curve; no point deviates from the curve by more than 5 % which, according to Harris (1970), is probably well within the accuracy of the machine. By comparison, the instrument at Madison gave readings which were in somewhat poorer agreement with the expected results: one point deviates by 17 % from the curve, though all but three of the measurements lie within 10 % of the curve. These discrepancies are rather disquieting, especially since we are unable to account for them. Nevertheless, in view of the very good agreement achieved between the other three instruments, we shall retain the assumption that the curve of figure 6 is a close approximation to $P_1(\dot{s})$.

7. The normal-stress distribution $p_{22}(r)$

In this section the discussion is to be restricted to the measurements of the normal stress $p_{22}(r)$ in the cone-and-plate apparatus with $c = 0$. Under these conditions the quantity $r(\partial p_{22}/\partial r)$ is a constant, with the result that p_{22} is expected to vary logarithmically with the radius. The measurements of the distribution $p_{22}(r)$ were made in apparatus IV, so that the results are liable to a systematic error arising from the use of cavities in the walls of the viscometer to determine p_{22} (see appendix A). This error is to be denoted by p_{H}.

For very deep and symmetrical cavities we shall make the assumption that the measuring error p_{H} is a function only of $\dot{s}$, the shear rate the undisturbed fluid would have at the surface of the viscometer and at the position of the cavity, were it nonexistent. Under this assumption it is evident that the observed stress $\bar{p}$‡ is related to the normal stress at the wall of the viscometer by the equation§

$$-p_{22} = \bar{p} + p_{\mathrm{H}}(\dot{s}). \tag{7.1}$$

In general, (7.1) cannot be justified on theoretical grounds, and accordingly we shall have to rely on *a posteriori* arguments based on the experimental evidence to give credence to its validity. However, that such a relation should hold is not unexpected on the basis of a number of careful experimental observations (see Greensmith & Rivlin 1953; Kaye *et al.* 1968; Tanner & Pipkin 1969; Pritchard 1970) all of which suggest that p_{H} for very deep, symmetric, cavities and slow

† The measurement of Δn is based on the assumption that the extinction angle χ' has been determined correctly; an error in χ' will in turn introduce an error to Δn. However, the refractive index n passes through extremal values at the angles χ' and $(90° + \chi')$ and so the measurement of Δn is not very sensitive to small errors in χ'. The error in the path length of the birefringent medium through which the light beam passes is assumed to be small: an error of 0.5 cm, which we believe would be unusual for this apparatus, introduces an error of only 2 %.

‡ $\bar{p}$ is the mean value of the equalizing pressures $p_{-\infty}$ (see appendix A) observed in both senses of rotation of the cone.

§ By virtue of the definition of the coordinate system the normal stress exerted *on* the wall is equal to $(-p_{22})$, thereby introducing the negative sign in (7.1).

flows, is independent of the shape of the cavity and is determined only by the local shear rate $\dot{s}$. The present measurements (see also § 8.3) support this contention.

In the cone-and-plate viscometer the shear rate $\dot{s}$ is independent of the radius and it follows from the assumption (7.1) that $\partial p_{22}/\partial r = -\partial \bar{p}/\partial r$. Thus, by virtue of (2.4), the experimentally determined quantity $r(\partial \bar{p}/\partial r)$ should specify the function $P_1 + 2P_2$. Now the measurements, of which examples are given in figure 10,† indicate that $\bar{p}$ varies logarithmically with the radius to a very high accuracy as suggested theoretically: typically, for six values of $\bar{p}(r)$, the quantity $r(\partial \bar{p}/\partial r)$ is specified to within a standard deviation of about 0.5 % of its magnitude, at the lower shear rates, and to within a standard deviation of about 1.0 % at the highest shear rate. (The increased variance at the higher shear rates appears to derive from a poorer inherent accuracy in determining the large values of $\bar{p}(r)$.)

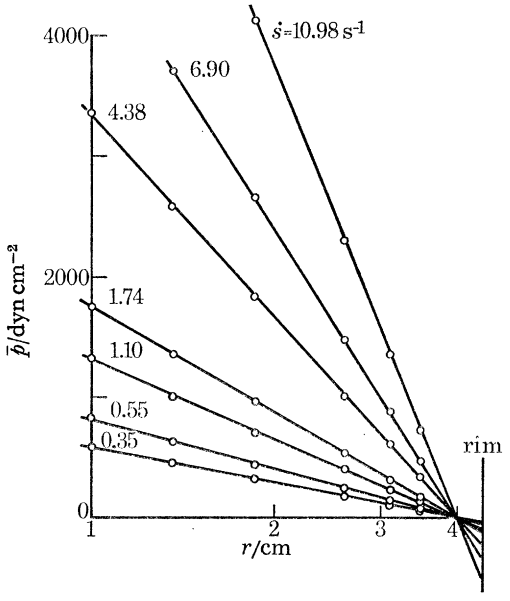

FIGURE 10. The normal-stress distribution $\bar{p}(r)$ in a cone-and-plate viscometer. The measurements were made on apparatus IV with the sea-of-liquid configuration; $\beta = 3.27°$.

Measurements of $r(\partial \bar{p}/\partial r)$ have been made on apparatus IV using three different cone angles with both the 'free boundary' and the 'sea-of-liquid' configurations sketched in figure 1. The results of these measurements are shown in figure 11 where it is seen that the data points deviate by a remarkably small amount from the approximate mean curve (which was drawn by eye): we shall accordingly assume that this curve is a good approximation to the material function $P_1 + 2P_2$, for the range of shear rates of the measurements.

In § 2.1 it was pointed out that a number of features could invalidate the cone-and-plate measurements. We shall now describe measurements undertaken to investigate experimentally some of these potential sources of error. One such source arises because the equations of motion are only satisfied approximately for viscometric flows between a cone and a plate, the neglected terms being of $O(\tan^2\beta)$ compared with terms of $O(1)$. Therefore, in an attempt to reveal the importance of the neglected terms, measurements have been made with three different cones.

† It is an interesting feature of figure 10 that $\bar{p}(r) = 0$ at very nearly the same value of r for all shear rates. This phenomenon was first noticed by den Otter (1967) and was also observed by Kaye *et al.* (1968). It is discussed in appendix C.

Theoretically, it is expected for a cone-and-plate viscometer that $p_{22} = (a + p_H) + b \ln r$, where a and b are constants for a given shear rate (see (2.7)), so that $\bar{p} = a + b \ln r$. The constant b represents the normal stress gradient $r(\partial\bar{p}/\partial r)$ and the quantities a and b together specify the normal thrust acting on the plate (to within a constant, of magnitude $\pi R^2 p_H$). Examples of the values determined for a and b are shown in figures 12 and 13. In figure 12 the shear rate is $1.74\,s^{-1}$ and we see for each cone that, with regard to b, the differences observed between the sea of liquid and the free-boundary condition are very small, except possibly for the case of the 5.67° cone. For two cones with the same angle $\beta (= 3.27°)$, but with different radii R, the values of b were found to be virtually indistinguishable. The mean value of b shown in figure 12 was determined by finding the mean value of b for each cone angle and then using the resultant six quantities to compute a mean.

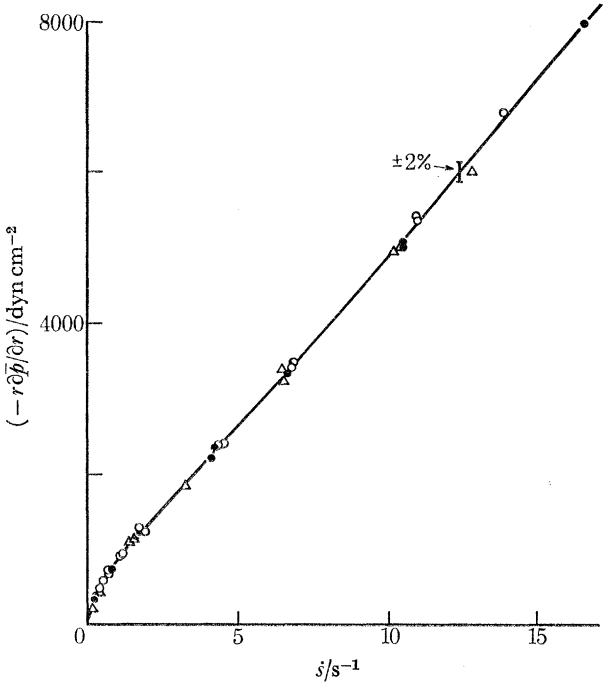

FIGURE 11. The normal-stress gradient $r(\partial\bar{p}/\partial r)$ in cone-and-plate viscometers using apparatus IV. ●, $\beta = 1.72°$; ○, $\beta = 3.27°$; △, $\beta = 5.67°$. ——, Approximate best fit of the data. The results include measurements made with a free boundary and with a sea of liquid at the rim of the cone.

When account is taken of the variability of the data at a given cone angle, it would appear that any systematic variations of b with the cone angle and with the boundary configuration constitute only a small influence at this shear rate; on the other hand, the results do suggest the existence of small differences between the various cones which we think merit further investigation. The measurements shown in figure 12 of the quantity a suggest, in the case of the free-boundary configuration, that the results are nearly compatible and that systematic differences are small. However, with the sea of liquid, the value of a for the 1.72° cone differs by about 6 % from the mean value of the measurements made with the free-boundary configuration and from the other measurements made with the sea of liquid; moreover, it is lower than the corresponding measurement with the 1.72° cone made with the free-boundary configuration.† This phenomenon was

† This result was completely unexpected, since it was thought that the presence of the sea of liquid would effectively lead to an increase in the hydrostatic pressure at the rim of the cone (cf. appendix C), thereby resulting in increased values of a.

observed with the 1.72° cone at all shear rates at which comparisons were made. It was not observed with the other two cones.

The results of measurements of a and b at a higher shear rate are shown in figure 13. The results are shown only for the free-boundary configuration. It is seen that both a and b show consistent measurements for the 1.72° and 3.27° cones. But, with the 5.67° cone, the values of both a and b

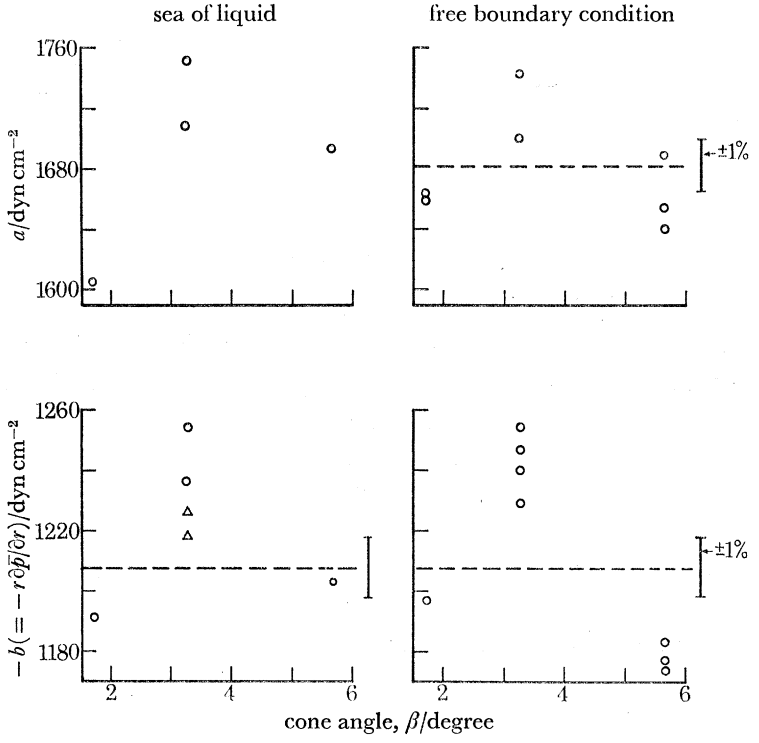

FIGURE 12. The quantities a and b (see § 7 for definition) determined as a function of the cone angle β at $\dot{s} = 1.74\,\mathrm{s}^{-1}$. ○, $R = 4.41$ cm; △, $R = 6.03$ cm. (Note: for $R = 6.03$ cm, and with the sea-of-liquid configuration, $a \sim 2100\,\mathrm{dyn/cm^2}$.)

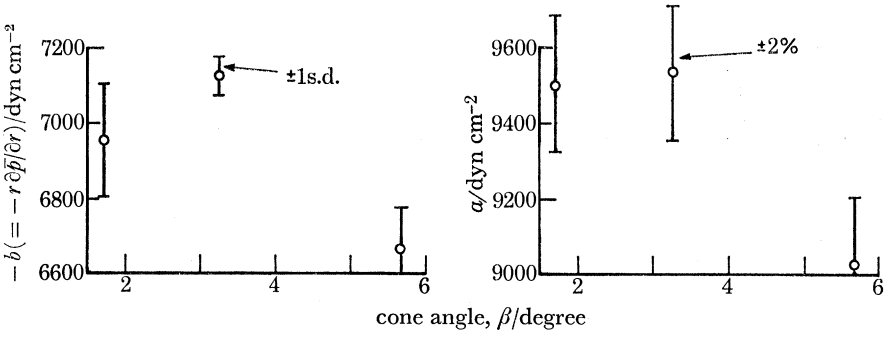

FIGURE 13. The quantities a and b (see § 7) determined as a function of the cone angle, with the free-boundary configuration. $\dot{s} = 14.5\,\mathrm{s}^{-1}$; $R = 4.41$ cm.

differ appreciably from the other results. At these high shear rates it is thought that such a difference may arise from the significant changes noticeable at the free boundary between the static state and the rotating state; the changes were not as evident with the 1.72° and the 3.27° cones.

Thus, taking these results into account we shall assume that the magnitude of the normal-stress gradient $r(\partial\bar{p}/\partial r)$, at a given shear rate, is represented by the mean value of all the measurements

at that shear rate (except possibly for the 5.67° cone at the higher shear rates). These factors have guided us in drawing an approximate curve-of-best-fit in figure 11 which, in view of the above results, we estimate should be accurate to within $\pm 2\,\%$. Therefore the curve of figure 11 should closely represent the material function $P_1 + 2P_2$ (that is, if assumption (7.1) is valid) so that, when taken in conjunction with the results of § 6, we are able to specify both material functions $P_1(\dot{s})$ and $P_2(\dot{s})$.

But to be able to account for some anomalous measurements of $P_1(\dot{s})$ from the concentric cylinders, and to interpret the results of the present section, a new function $p_{\mathrm{H}}(\dot{s})$ has been introduced. We shall now determine this new function and check it with a number of independent measurements.

8. The error arising from the holes

8.1. *Determination of* $p_{\mathrm{H}}(\dot{s})$

In determining $P_1(\dot{s})$ and $P_2(\dot{s})$ no knowledge of p_{H} was required. The measurement that p_{H} could have affected was that of the normal-stress gradient $r(\partial p_{22}/\partial r)$ in the cone-and-plate apparatus, but the influence of p_{H} vanished there by virtue of assumption (7.1). However, measurements of the normal-stress distribution $p_{22}(r)$ in the plate-and-plate viscometer should, according to (7.1), be influenced by p_{H} since the shear rate is now a function of the radius. To demonstrate this result, we see from (2.16) that the normal-stress distribution $p_{22}(\dot{s}) - p_{22}(0)$ is specified by the known functions $P_1(\dot{s})$ and $P_2(\dot{s})$, so that a 'theoretical' stress distribution may be compared with the measured distribution $\bar{p}(0) - \bar{p}(\dot{s})$. Such a comparison is shown in figure 14 and the disparity between the prediction and observation is evident.† Indeed the difference between these two results is a direct measure of p_{H}: it follows from (2.16) and assumption (7.1) that

$$p_{\mathrm{H}}(\dot{s}) - p_{\mathrm{H}}(0) = (\bar{p}(0) - \bar{p}(\dot{s})) - P_2(\dot{s}) - \int_0^{\dot{s}} (P_1 + P_2)\, \zeta^{-1}\, \mathrm{d}\zeta, \tag{8.1}$$

where the relation between $\dot{s}$ and the radius is determined from (2.3). Now the discussion of the physical origin of p_{H} (see appendix A) indicates that $p_{\mathrm{H}}(0) = 0$: near the cavity there is no motion of the fluid and the measurement becomes the determination of a hydrostatic pressure. Thus (8.1) may be used to evaluate $p_{\mathrm{H}}(\dot{s})$.‡

The measurements of $\bar{p}(0) - \bar{p}(\dot{s})$ shown in figure 14 indicate a fairly large scatter in the data, especially at the higher shear rates. It is believed that almost all of this scatter arises from the

† It was mentioned in the Introduction that this test had previously been carried out by Markovitz (1965 *a*) who obtained agreement between the measurements and the prediction. Markovitz, however, determined P_1 from measurements using concentric cylinders and his values of P_1 are influenced by p_{H}. Thus for Markovitz's fluid the influence of p_{H} on both sides of (2.16) must have been nearly the same, thereby giving an illusory agreement. A repetition of Markovitz's test, on the present fluid, is given in appendix B.

‡ If the lowest shear rate at which the functions P_1 and P_2 have been measured is α, then the integral of (8.1) can be evaluated graphically only over the range $[\alpha, \dot{s}]$. Therefore the right-hand side of (8.1) is determined only up to a constant C_0 given by

$$\int_0^{\alpha} (P_1 + P_2)\, \zeta^{-1}\, \mathrm{d}\zeta$$

which we are unable to specify experimentally. A crude estimate of C_0 has been made from the function

$$\phi(\dot{s}) = \int_{\alpha}^{\dot{s}} (P_1 + P_2)\, \zeta^{-1}\, \mathrm{d}\zeta$$

by arbitrarily specifying that $C_0 = \phi(2\alpha)$. C_0 is thought to be of the order of 50 dyn/cm². A similar procedure will be used in other parts of the paper without further comment.

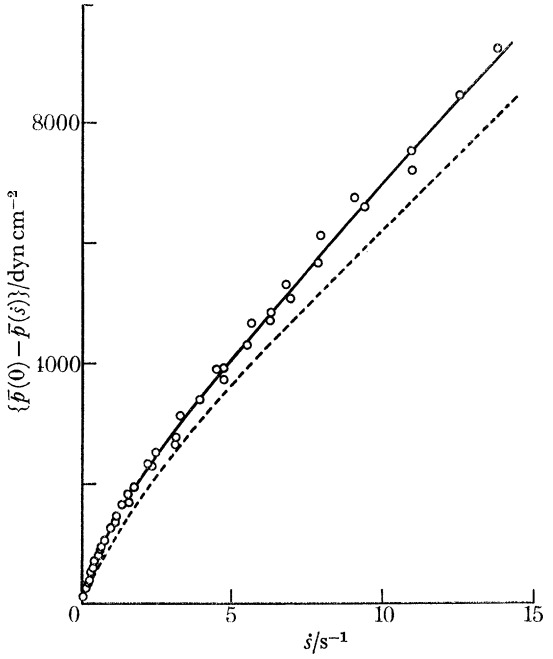

FIGURE 14. A demonstration of the existence of the function p_{H}. ○, Direct measurement of $\bar{p}(0)-\bar{p}(\dot{s})$ for parallel plates, in apparatus IV with a sea of liquid; (the measurements were made at five values of Ω and for plate separations, c, of 0.250 cm and 0.132 cm; $R = 4.41$ cm). – – – –, Function $P_2(\dot{s}) + \int_0^{\dot{s}} (P_1+P_2)\,\zeta^{-1}\mathrm{d}\zeta$.

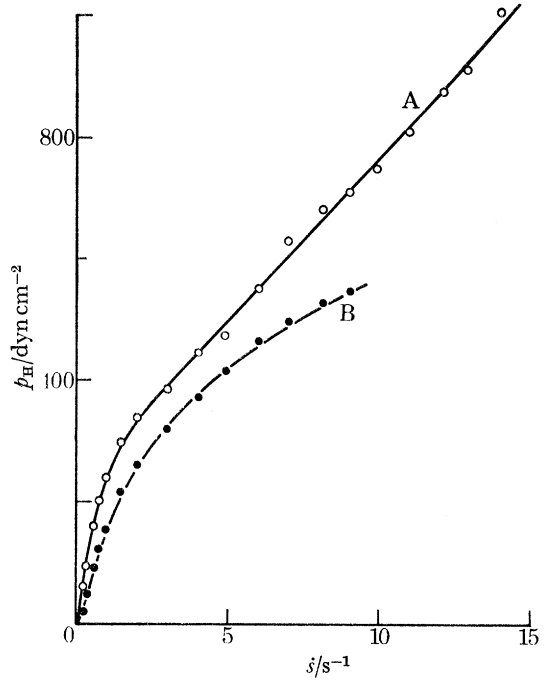

FIGURE 15. The hole measuring error, $p_{\mathrm{H}}(\dot{s})$. ○, Determined via (8.1) from measurements of $\bar{p}(0)-\bar{p}(\dot{s})$ by parallel plates. ●, Determined via (8.2) from $r(\partial\bar{p}/\partial r)$ in the plate-and-plate apparatus.

determination of $\bar{p}(0)$ since a small error in $\bar{p}(0)$ influences systematically a number of data points. For example, a small error in setting the measuring hole at $r = 0$ would introduce a large error in $\bar{p}(0)$; also the large magnitudes of the stresses encountered at $r = 0$ were difficult to measure in these experiments because of hysteresis effects in the transducers. The data of figure 14 have been taken from measurements made at six different angular velocities of the upper plate and at different gap widths between the plates. At the lower shear rates the superposition of the data is quite good, but at the higher shear rates it is less accurate. Yet the deviation of each set of data from the mean curve suggested no obvious trends, so we feel justified in taking the mean curve to be a good approximation to $\bar{p}(0) - \bar{p}(\dot{s})$. The difference between the two curves of figure 14 is shown in figure 15 (curve A). It would be difficult to give a fair estimate of the accuracy of this measurement of p_{H}.

Also shown in figure 15 is a second, less reliable, determination of $p_{\mathrm{H}}(\dot{s})$ made from the plate-and-plate measurements. On integrating (2.15) and using (7.1) it follows for parallel plates that

$$p_{\mathrm{H}}(\dot{s}) = -P_2(\dot{s}) - \int_0^{\dot{s}} \left[(P_1 + P_2) + r \frac{\partial \bar{p}}{\partial r} \right] \zeta^{-1} \, \mathrm{d}\zeta. \tag{8.2}$$

Some examples of measurements of $\bar{p}(r)$ in the plate-and-plate viscometer (apparatus IV) are given in figure 16 and it is seen that, near the rims of the platens, $\bar{p}$ is nearly logarithmic in r.

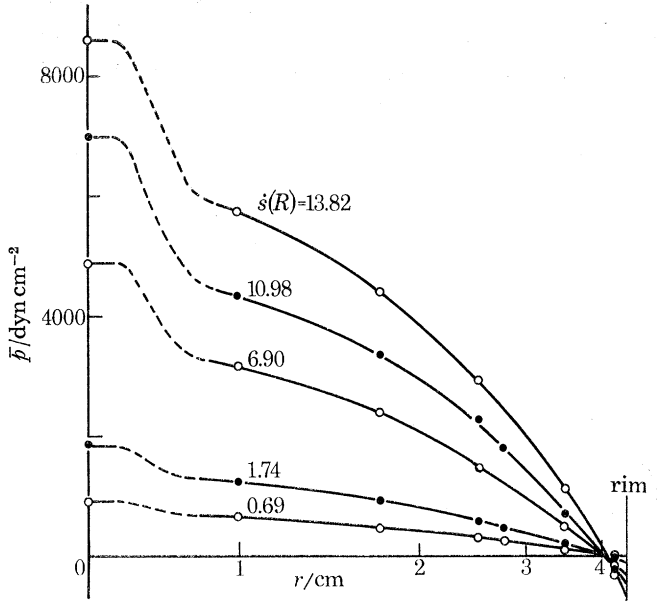

FIGURE 16. Measurements of the stress $\bar{p}(r)$ in the plate-and-plate viscometer of apparatus IV, for various values of $\dot{s}(R)$. The plate separation $c = 0.250$ cm. $R = 4.41$ cm.

Thus the quantity $r(\partial \bar{p}/\partial r)$ may be found approximately by fitting straight lines to the data points near the rim; usually only the two outermost points were used. The values of p_{H} then determined via (8.2) are shown in figure 15 (curve B), and considering the inherent unreliability of this method (namely the use of two experimental points to define a derivative), the similarity of the two curves is encouraging: the difference of 170 dyn/cm^2 between the two curves at $\dot{s} \sim 10\,\mathrm{s}^{-1}$ could easily arise from the determination of $r(\partial \bar{p}/\partial r)$. But more weight should be attached in what follows to curve A than to curve B.

In figure 17 the ratio p_H/P_1 is plotted as a function of the shear rate. The exact theory for slow, two-dimensional, flows of a second-order fluid and the approximate theory for slow flows of a second-order fluid past a circular hole (see Higashitani & Pritchard 1971 and appendix A) are also shown in figure 17. Even though the measurements were made at shear rates well outside the range of validity of the second-order fluid approximation the theoretical values for p_H are in good overall agreement with the experimental results. Indeed at shear rates of about $1\,s^{-1}$, where the largest discrepancies occur, an error of less than $50\,dyn/cm^2$ in the determination of p_H would account for the differences. Such errors are thought to be well within the experimental accuracy of the measurements.

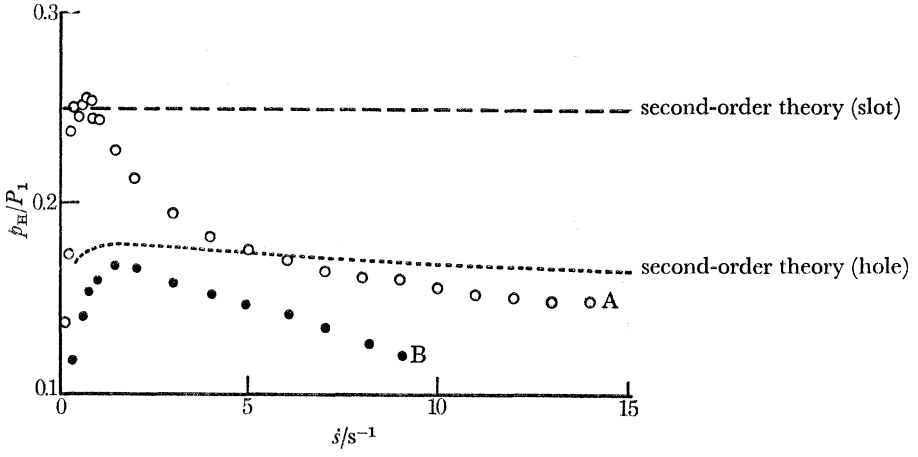

FIGURE 17. The value of the ratio p_H/P_1. ○, From the measurements of $\bar{p}(0)-\bar{p}(\dot{s})$; ●, from the measurements of $r(\partial\bar{p}/\partial r)$.

8.2. *The normal stress at the rim*

An independent check of p_H may be made from measurements of the normal stress $\bar{p}$ at the rim of the cone-and-plate viscometer. From equation (2.5) and assumption (7.1) it follows that

$$\bar{p}(R) = -p_H(\dot{s}) - P_2(\dot{s}). \tag{8.3}$$

Experimental estimates of $\bar{p}(R)$ may be obtained from the results discussed in § 7 by extrapolating the logarithmic distribution of $\bar{p}(r)$ to the rim, as indicated in figure 10. However, as indicated in § 7, the value of $\bar{p}(R)$ is dependent upon the conditions at the rim of the cone especially when the sea-of-liquid configuration is being used. In view of this complication a detailed set of measurements of $\bar{p}(R)$ was made for all available conditions at the outer boundary: the results are shown in figure 18.

The measurements made with the free-boundary configuration are indicated by the dark spots and are seen to lie in a fairly narrow band, with the exception of the measurements with the 5.67° cone at the higher shear rates. The deviation of these latter measurements was discussed in § 7. Using the sea-of-liquid configuration with the 1.72° cone the results for $\bar{p}(R)$ are in good agreement with the free-boundary measurements. With the 3.27° and 5.67° cones in a sea of liquid the values of $\bar{p}(R)$ are smaller in magnitude (i.e. $\bar{p}(R)$ increases) than the free-boundary measurements because of an effective increase in the hydrostatic pressure at the rim arising from the Weissenberg effect at the cylindrical surface of the rotating platen. The effect is particularly noticeable with the 5.67° cone at the higher shear rates; a rough quantitative account of its influence is given in appendix C.

Equation (8.3) also applies at the rim of the plate-and-plate viscometer if the boundary condition (2.2) is assumed. Accordingly some measurements of $\bar{p}(R)$ obtained with parallel plates in a sea of liquid are included in figure 18: those shown are for a plate separation, c, equal to the gap at the rim of the 3.27° cone (so that $\dot{s}(R)$ is the same in both instruments at the same value of Ω) and it is seen that the results are in good agreement with those for the 3.27° cone rotating in a sea of liquid.

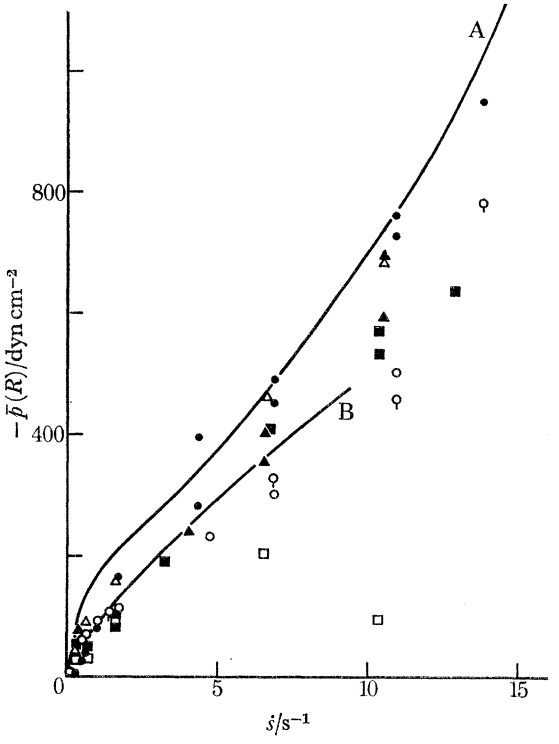

FIGURE 18. The stress $\bar{p}(R)$ at the rim of the cone-and-plate viscometer (apparatus IV) for various cone angles and various conditions at the outer boundary. Curves A and B are values of $\bar{p}(R)$ deduced from the corresponding measurements of p_H shown in figure 15. (N.B. The measurements from the parallel plates were taken with a gap between the plates equal to the gap at the rim of the 3.27° cone.)

cone angle (°)	0	1.72	3.27	5.67
sea of liquid	♀	△	○	□
free boundary		▲	●	■

The two curves shown in figure 18 are the predictions of $\bar{p}(R)$ derived from (8.3) in which the values of p_H shown in figure 15 were used. The overall agreement between these curves and the experimental results provides a good confirmation of the estimates of p_H. It was anticipated that the 1.72° and the 3.27° cones used with the free-boundary configuration would most nearly approach the theoretical conditions, in which case curve B gives too small a value for $|\bar{p}(R)|$. On the other hand curve A is in very good agreement with the data, except at shear rates below about 5 s^{-1} where it appears to predict slightly too large a value for $|\bar{p}(R)|$. These discrepancies of about 50 dyn/cm^2 are thought to lie within the experimental accuracy of the measurements.

Having thus determined and checked the function $p_H(\dot{s})$ it now remains to see if the same function can be used to resolve the anomalous values of $P_1(\dot{s})$ deduced from the measurements made with the concentric cylinders (apparatus VI).

8.3. *Concentric-cylinders measurements*

The normal-stress difference $P_1(\dot{s})$ may be determined from measurements of the normal stresses p_{22} acting on the inner and outer cylinders (cf. § 2.3). But the preceding discussion indicates that the methods used to measure p_{22} will give invalid results unless the data are corrected for the hole measuring error p_H. It is, however, more convenient to use the measurements from the concentric cylinders to check the results for p_H. Thus, on substituting (7.1) in (2.22) it follows that

$$p_H(\dot{s}_i) - p_H(\dot{s}_o) = (\bar{p}_o - \bar{p}_i) + \frac{1}{2}\int_{\sigma_i - \delta}^{\sigma_i} P_1(\sigma)\, d\sigma, \tag{8.4}$$

where the subscripts i, o refer to the inner and outer cylinder respectively, and $\sigma = \ln p_{21}$. In (8.4) it is assumed for simplicity that the inertial correction discussed in § 3 (VI) is incorporated in the term $(\bar{p}_o - \bar{p}_i)$.

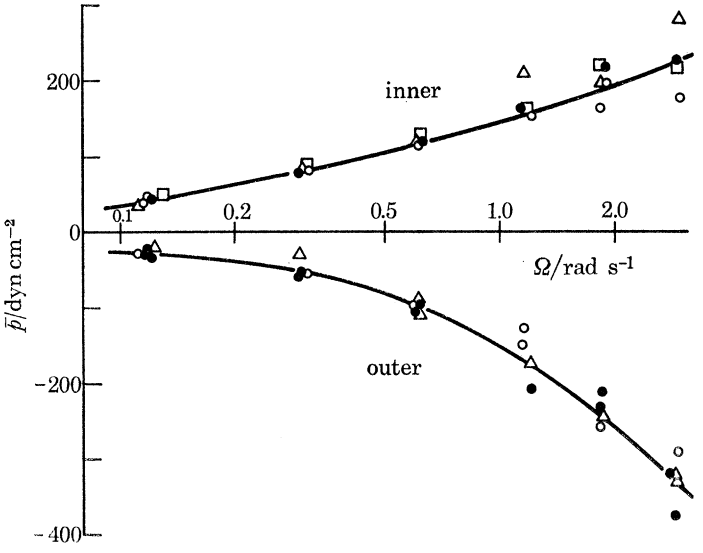

FIGURE 19. The stress $\bar{p}$ measured at the inner and outer walls of the concentric cylinders, apparatus VI. The ratio, κ, of the cylinder radii is 0.577; $R_i = 6.840$ cm. The data points represent measurements made with holes of diameter d. △, $d = 0.102$ cm; ○, $d = 0.204$ cm; □, $d = 0.305$ cm; ●, $d = 0.508$ cm.

The assumption that the measuring error p_H is independent of the dimensions of the cavity, for very deep holes, and is determined entirely by the local, unperturbed, value of the shear rate near the cavity entrance has been checked fairly extensively in the cone-and-plate and plate-and-plate viscometers (cf. § 7). However, for measurements made with the concentric-cylinders apparatus, the possibility arises that p_H may depend upon the size of the cavity since a new length scale, namely the cylinder radius, has been introduced: indeed, some tentative measurements of Broadbent (see Pritchard 1970) using two different cavities suggest this to be the case. Consequently a detailed experimental investigation into this possibility was carried out and it is now believed, on the basis of the present results, that p_H is in fact independent of the dimension of the cavity when it is very deep.

The current measurements were made with four different pairs of inner and outer cylinders. Each inner cylinder was equipped with measuring holes of four sizes and each outer cylinder had three holes of differing size so that a wide range of cavity dimensions was employed.† Yet no

† In the course of these measurements the ratio $d/(R_o - R_i)$, where d is the diameter of the measuring hole, varied between 0.020 and 0.346; the ratio d/R_i lay between 0.012 and 0.074.

systematic variation of $\bar{p}$ with the cavity dimension was observed in any of the measurements, an example of which is given in figure 19. The three other sets of data are of a similar nature to that shown in figure 19 (with the exception that one set displays more scatter than occurs in the other measurements), so that we feel justified in using approximate curves that fit the data in the mean to represent the values of $\bar{p}_i$ and $\bar{p}_o$ in further computations. Moreover it is felt that these results provide strong evidence in support of assumption (7.1) that the function $p_H = p_H(\dot{s})$. Although

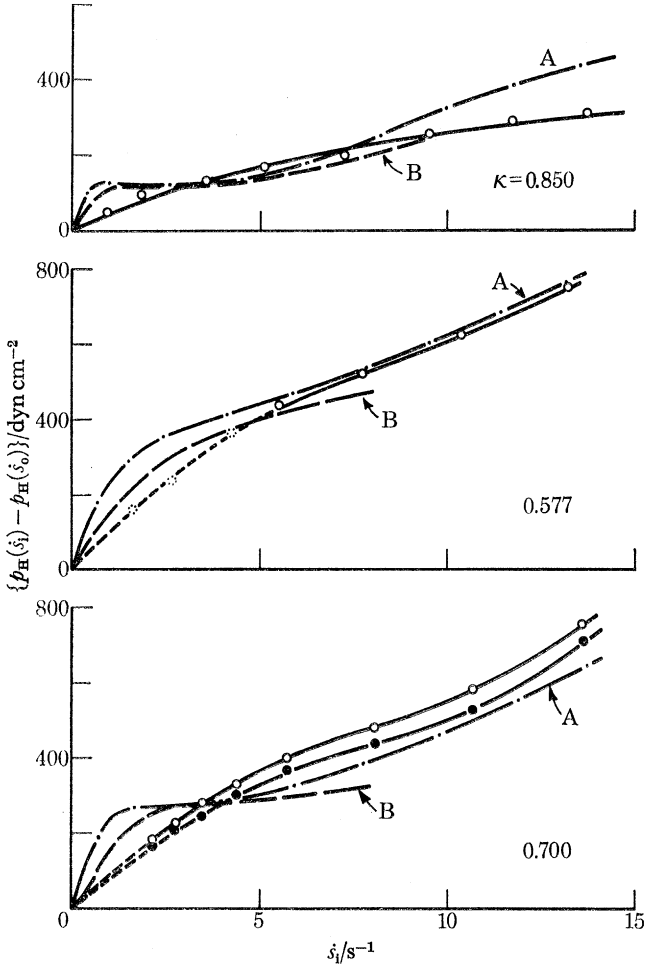

FIGURE 20. The hole error $p_H(\dot{s}_i) - p_H(\dot{s}_o)$ determined from the concentric-cylinders measurements. Curves A and B are estimates of the same quantity made from the respective curves of figure 15. $\kappa = 0.700$: ○, $R_i = 8.303$ cm; ●, $R_i = 6.840$ cm. $\kappa = 0.577$: ○, $R_i = 6.840$ cm. $\kappa = 0.850$: ○, $R_i = 8.303$ cm.

these findings are at variance with the above-mentioned results of Broadbent, the resolution of the conflict most probably lies in the very large differences Broadbent observed in one of the sets of measurements between the clockwise and the anticlockwise senses of rotation of the inner cylinder; $\bar{p}_i$ was taken to be the mean value of the two readings. This anomaly in Broadbent's measurements is thought to occur because the axis of the measuring hole did not lie exactly along a radial direction. Accordingly, new cylinders were manufactured for the present experiments in which great care was taken with the drilling of the holes, with the result that the measurements in each sense of rotation were in good agreement.

Following these preliminaries we are in a position to evaluate the right-hand side of (8.4), for a given value of κ, thereby estimating $p_H(\dot{s}_i) - p_H(\dot{s}_o)$. The results of the computations for each of the sets of measurements made with apparatus VI are shown in figure 20. The two sets of measurements made at $\kappa = 0.700$ give values of $p_H(\dot{s}_i) - p_H(\dot{s}_o)$ differing at most by 50 dyn/cm², which we anticipate to be well within the experimental accuracy.† For shear rates $\dot{s}_i$ greater than about $4\,s^{-1}$ these results are in good agreement with the value of $p_H(\dot{s}_i) - p_H(\dot{s}_o)$ derived from curve A of figure 15, especially if one considers that both methods of determining $p_H(\dot{s}_i) - p_H(\dot{s}_o)$ are liable to sizeable experimental errors. The results for $\kappa = 0.577$ show very good agreement between the measurements of $p_H(\dot{s}_i) - p_H(\dot{s}_o)$ and the value deduced from figure 15 (curve A), except for shear rates $\dot{s}_i$ less than about $5\,s^{-1}$; but in order to evaluate the right-hand side of (8.4) at these shear

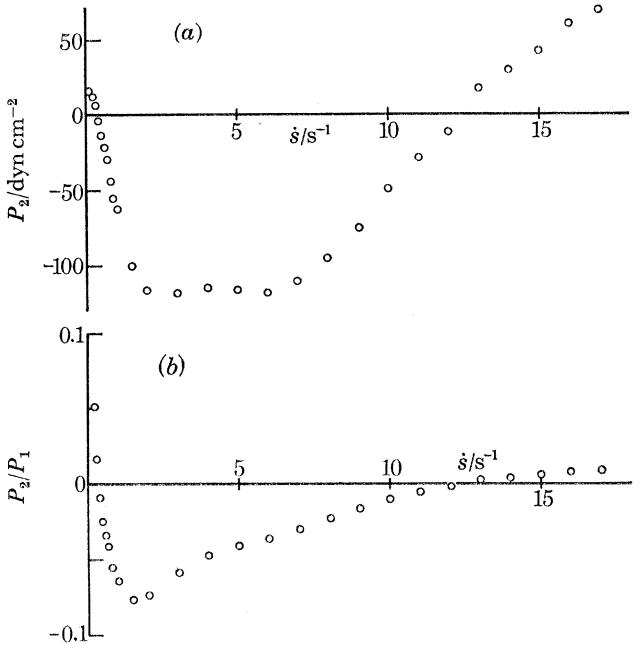

FIGURE 21. The secondary normal-stress difference $P_2(\dot{s})$. (*a*) The value of $P_2(\dot{s})$ determined from the curves of figures 6 and 11. (*b*) The ratio of $P_2(\dot{s})$ to $P_1(\dot{s})$.

rates the function $P_1(\dot{s})$ was extrapolated beyond the range of shear rates over which it had been measured. The uncertain part of the curve is shown as a dashed line. For $\kappa = 0.850$ the agreement between the measurements and the predictions from the p_H values is not as successful as in the two other cases, but because of technical difficulties encountered with the electronic part of the measuring system at the inner cylinder, the reproducibility of the results was poor and this set of measurements is less reliable than the other cases; even so, the agreement between the estimates of $p_H(\dot{s}_i) - p_H(\dot{s}_o)$, for values of $\dot{s}_i$ in excess of $4\,s^{-1}$, is fairly good.

On the other hand, when $\dot{s}_i < 4\,s^{-1}$, there is a small discordance between the measurements of $p_H(\dot{s}_i) - p_H(\dot{s}_o)$ and the predictions made from figure 15, and since the nature of this disparity is the same in each case there would appear to be some small systematic errors in the data. These

† It is difficult to give a good estimate of the experimental errors associated with these measurements, but it is clear from the reproducibility of the readings of $\bar{p}_i$ and $\bar{p}_o$ shown in figure 19 that an error of ± 10 dyn/cm² is not unlikely in either of these measurements. If we assume a similar accuracy for $p_H(\dot{s}_i)$ and $p_H(\dot{s}_o)$ we see that (8.4) cannot be expected to balance to within ± 40 dyn/cm², without taking into consideration the accuracy of the numerical integration required in the equation. In reality the accuracy of the measurements, especially those of p_H, is less precise than this.

discrepancies are consistent with the suggestion made in § 8.2 that the value of p_H indicated in figure 15 (curve A) is slightly too large at shear rates up to about $5\,s^{-1}$.

9. The secondary normal-stress difference

From the measurements of P_1 (§ 6) and of $P_1 + 2P_2$ (§ 7) the secondary normal-stress difference P_2 is readily found and is shown in figure 21 (*a*). In figure 21 (*b*) the ratio $P_2(\dot{s})/P_1(\dot{s})$ is shown. It is difficult to estimate the accuracy of this measurement of P_2, but if we assume that both P_1 and $P_1 + 2P_2$ have been correctly determined to within 2 %, the error possible in P_2 is $\pm 40\,dyn/cm^2$ at $\dot{s} = 1\,s^{-1}$, $\pm 120\,dyn/cm^2$ at $\dot{s} = 5\,s^{-1}$ and $\pm 280\,dyn/cm^2$ at $\dot{s} = 15\,s^{-1}$.

Because of the good self-consistency of all the experimental results discussed above, we place a high degree of confidence in the measurement of P_2 shown in figure 21. It is interesting that these results suggest that P_2 is an order of magnitude smaller than P_1 and, if the results are taken at face value, that $P_2(\dot{s})$ changes from a negative quantity at low shear rates to a positive quantity at shear rates in excess of about $12\,s^{-1}$. But the errors inherent in the measurement could easily mask this latter characteristic of P_2.

Having now established an estimate of $P_2(\dot{s})$ we shall proceed to compare it with other measurements of the function.

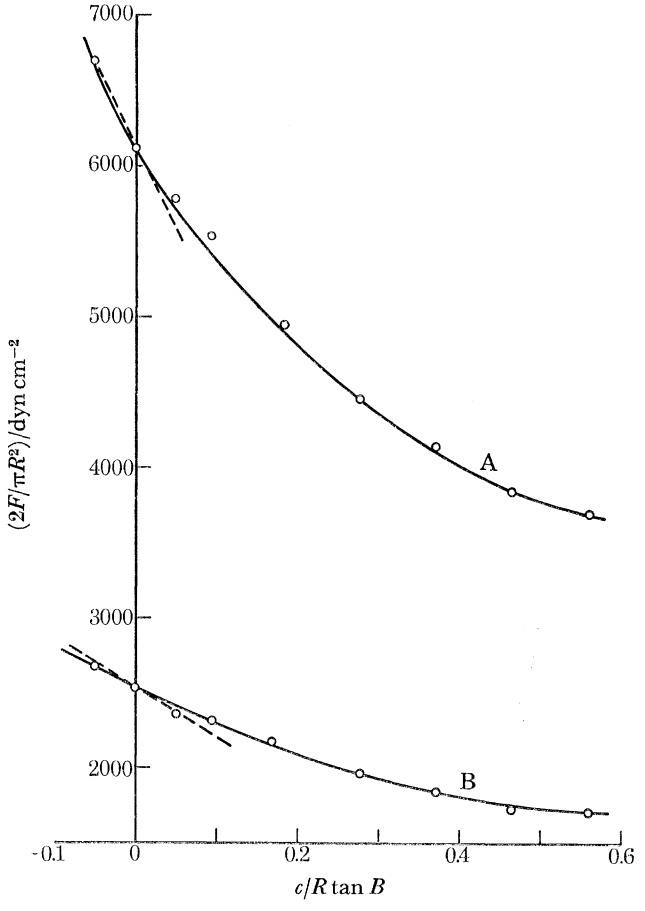

Figure 22. Examples of the dependence of the normal force F on the separation c in the cone-and-plate viscometer, apparatus I. A: $\dot{s}(R) = 12.62\,s^{-1}$. B: $\dot{s}(R) = 4.22\,s^{-1}$. The dashed lines indicate the gradient $(\partial F/\partial c)_{c=0}$ needed for the Jackson & Kaye method of determining P_2 to give agreement with the results of figure 21.

9.1. *The Jackson & Kaye method*

A method of determining P_2, proposed by Jackson & Kaye (1966), is to measure the normal thrust F acting on the plate of a cone-and-plate viscometer for various values of the parameter c (see figure 1) and thereby to determine the gradient $(\partial F/\partial c)_{c=0}$; $P_2(\dot{s})$ may then be deduced from equation (2.12).

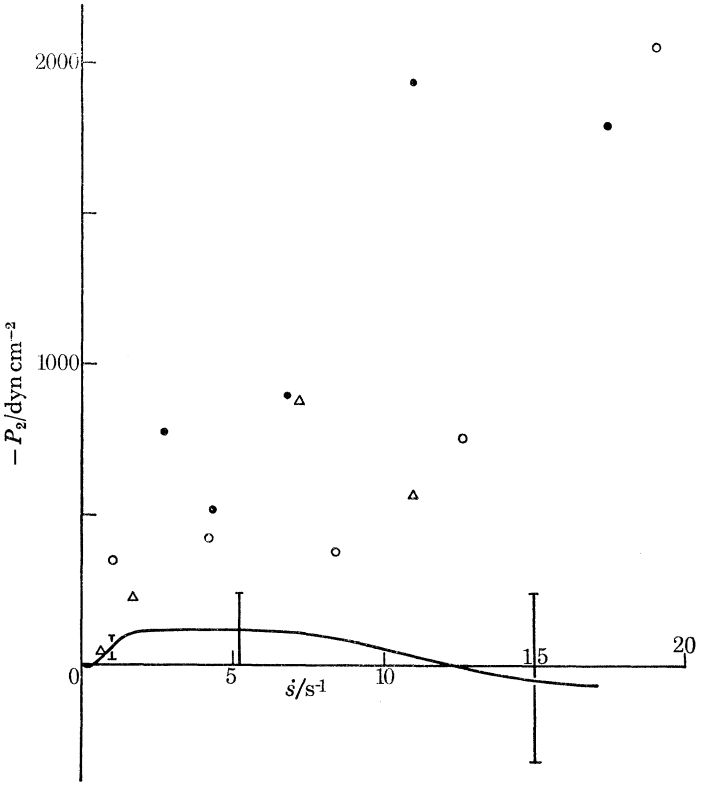

FIGURE 23. Estimates of $P_2(\dot{s})$ from the Jackson & Kaye method are compared with the estimate of P_2 of figure 21. ○, Measurements made on apparatus I; ●, measurements made on apparatus II, △, approximate values of P_2 obtained from apparatus IV.

Two examples of the measurements of $F(c)$ are shown in figure 22, and it was from the smooth curves approximately representing these data points that the slopes $(\partial F/\partial c)_{c=0}$ were estimated. But to evaluate $P_2(\dot{s})$ from (2.12) the quantity $\mathrm{d}P_1(\dot{s})/\mathrm{d}\ln\dot{s}$ is needed, and this was derived from the measurements of $P_1(\dot{s})$ in a similar manner. However, in determining $\mathrm{d}P_1/\mathrm{d}\ln\dot{s}$ a check on the accuracy of the differentiation may be carried out by plotting P_1 as a function of both $\dot{s}$ and $\ln\dot{s}$ and then estimating the gradient $\mathrm{d}P_1/\mathrm{d}\ln\dot{s}$ from two different curves. The values of $\mathrm{d}P_1/\mathrm{d}\ln\dot{s}$ found by these means differed by less than 2 % in all cases, suggesting that the estimates are not too inaccurate. The values of P_2 obtained from apparatus I by this procedure are indicated by the circles of figure 23. The results are not in agreement with the estimate of P_2 given in figure 21. Unfortunately the errors associated with the determination of P_2 by the Jackson & Kaye method are likely to be fairly large, and rather difficult to estimate with any certainty. Accordingly, drawn in figure 22 is the gradient $\partial F/\partial c$ that would make the value of P_2 from the Jackson & Kaye method agree with the value of P_2 of figure 21, and it is seen that only a small change in $\partial F/\partial c$ is needed to account for the large discrepancy in figure 23.

An independent measurement of P_2 using the method of Jackson & Kaye was made on apparatus II at Madison by Dr E. K. Harris, Jr. In this case, however, polynomial curves were 'fitted' to the data† by the method of least squares, and the appropriate gradients deduced from these curves. The resultant values of P_2 are shown in figure 23; they do not agree with the estimate of P_2 given in figure 21.

Yet another estimate of P_2 by the method of Jackson & Kaye was made, in this case using apparatus IV. The normal-stress distribution $p_{22}(r)$ was determined‡ at various values of c, over an annular section of the plate, from which the normal thrust F acting on that annular region was calculated. Then approximate values of P_2 were found from (2.11) by neglecting the term $(2R_1/R)\,\mathrm{d}P_2/\mathrm{d}\ln\dot{s}$. Estimates of F were made at six values of c lying in the range

$$-0.040 \leqslant c/R\tan\beta \leqslant 0.101$$

and a straight line, chosen by the method of least squares, was used to represent the data points. The standard deviation of the regression was less than 1 % in each case, and consequently the slope of this line was assumed to be a good approximation to $(\partial F/\partial c)_{c=0}$. The estimates of P_2 thus determined are also shown in figure 23: they are not in accordance with the value of P_2 from figure 21, and, if anything, they confirm the other estimates of P_2 found by the Jackson & Kaye method.

A further confirmation of the results for P_2 obtained by the Jackson & Kaye method is described in appendix D.

9.2. *The Marsh & Pearson method*

This method of determining P_2 is similar to that of Jackson & Kaye, but the force F and the quantity $\partial F/\partial c$ may be measured at any given value of c, with the exception of $c = 0$; P_2 is then computed from (2.14).

By following similar procedures to those outlined in § 9.1 the values of F and

$$m(=-\partial\ln F/\partial\ln c)$$

were determined for a chosen value of c. The resultant values of P_2, computed for three different values of c are shown in figure 24: the results are neither in agreement with each other nor are they in agreement with the estimate of P_2 of figure 21. A possible explanation of this phenomenon is that a small systematic error in the measurement of $(P_1-(2+m)\,F/\pi R^2)$ will in effect be magnified when it is multiplied by the factor $(1+R\tan\beta/c)$ (cf. (2.14)). For example, with the measurements made at $c/R\tan\beta = 0.093$ a systematic error of only 1 % in either P_1 or in $(2+m)\,F/\pi R^2$ would result in a systematic error in P_2 of about 1000 dyn/cm² at a shear rate of 15 s^{-1}; even at the largest value of $c/R\tan\beta$ used in the experiments the magnification factor is about 4. Thus, in view of the large errors associated with this procedure, it is felt that the estimates of P_2 made at the widest separation are in as close an agreement with the estimate of figure 21 as could be expected. On the other hand, the estimates of P_2 made at the smaller separations are in such poor agreement with the estimate of figure 21 that it would appear as though some systematic influence is giving rise to the disparity.

An estimate of P_2 by the Marsh & Pearson method was also made at Madison using the curve-fitting techniques outlined in § 9.1. The results of these measurements are shown in figure 24 and again the results suggest that P_2 has a magnitude far in excess of that suggested in figure 21.

† It should be noted that the measurements of $P_1(\dot{s})$ made at Madison (see figure 9) were used in this computation. No measurements of $F(c)$ were made for values of $c < 0$.

‡ The stress p_{22} was determined from measurements of $\bar{p}$ and the function p_H of figure 15 (curve A) using assumption (7.1).

PHILOSOPHICAL TRANSACTIONS OF THE ROYAL SOCIETY A MATHEMATICAL, PHYSICAL & ENGINEERING SCIENCES

9.3. *The Kotaka* et al. *method*

As a special case of the Marsh & Pearson method the plate-and-plate viscometer may be used to deduce P_2. In this case $\beta = 0$ so that the factor $(1 + R\tan\beta/c)$, which greatly magnified the experimental errors in § 9.2, is of less importance and the estimate of P_2 is correspondingly more accurate. This method of determining P_2 was first proposed by Kotaka *et al.* (1959).

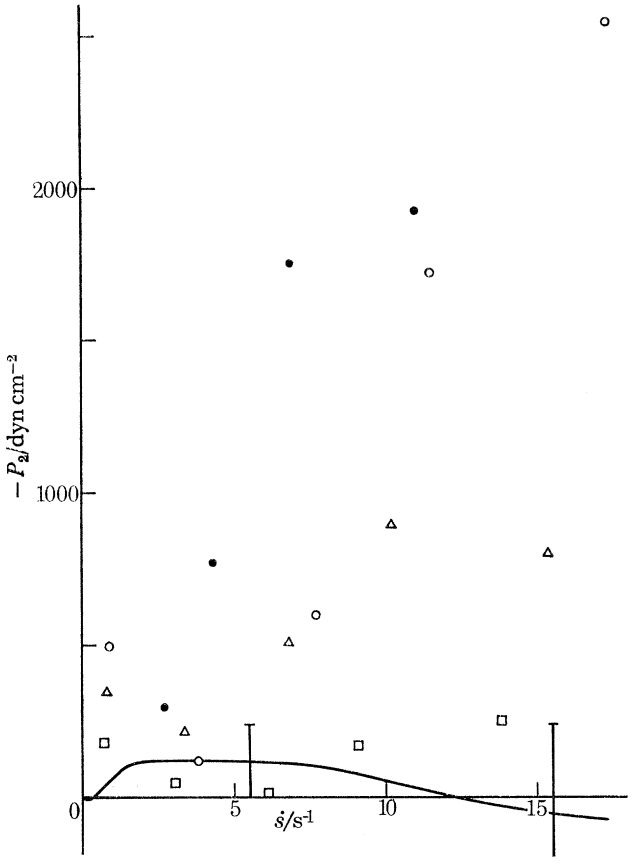

FIGURE 24. Estimates of $P_2(\dot{s})$ from the Marsh & Pearson method are compared with the estimate of P_2 of figure 21. ○: $c/R\tan\beta = 0.093$; apparatus I. △, $c/R\tan\beta = 0.228$, apparatus I; □, $c/R\tan\beta = 0.358$, apparatus I: ●, measurements made on apparatus II.

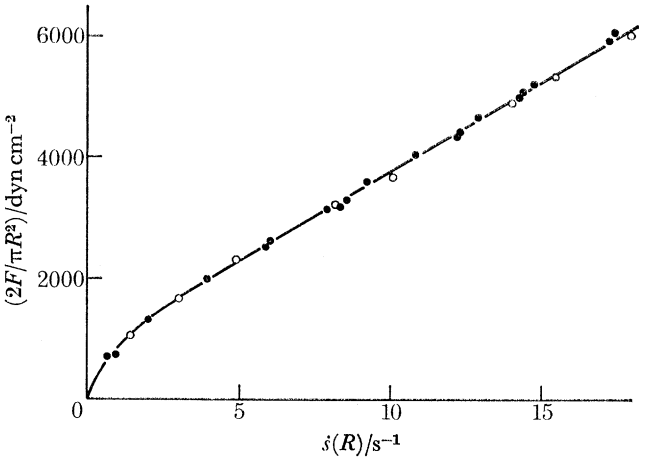

FIGURE 25. The normal force F in the plate-and-plate viscometer, apparatus I. ○, $c = 0.175$ cm; ●, $c = 0.219$ cm.

For the plate-and-plate viscometer it follows from (2.17) that the normal force F acting on the plates is, for a given material, determined by the shear rate at the rim of the plates and is independent of the separation, c, between the plates. That this is observed in practice is shown in figure 25 where, for two different plate separations, the values of F agree to within the experimental scatter of the data. Similar results had been obtained in § 8.1 in connexion with the measurements of the distribution of the normal stress $p_{22}(r)$. From the smooth curve used to represent the data of figure 25 the gradient $\partial F/\partial \dot{s}(R)$ was determined and $P_2(\dot{s}(R))$ accordingly estimated via (2.18), the results of which are shown in figure 26. Again the estimate of P_2 is not in good agreement with that of figure 21, but in view of the errors associated with the experiments the discrepancy is not seen to be significant.

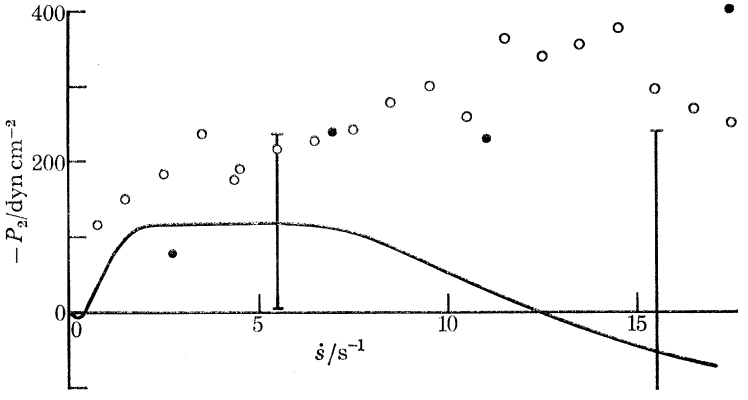

FIGURE 26. Estimates of $P_2(\dot{s})$ from the method of Kotaka *et al.* are compared with the estimate of P_2 of figure 21. ○, Apparatus I; ●, apparatus II.

Also shown in figure 26 are the results of some measurements made on apparatus II at Madison. In order to estimate P_2 in this case, the function $F(\dot{s}(R))$ was approximated by a polynomial expansion in $\dot{s}(R)$ from which the gradient $\partial F/\partial \dot{s}(R)$ was determined.

The two estimates of P_2 made using the method of Kotaka *et al.* are in good agreement with each other.

9.4. *Discussion*

In § 9 have been presented measurements of P_2 made by four different methods. The results of the first of these measurements were derived from the data of §§ 6, 7 and are given in figure 21. It was assumed throughout § 9 that this data represents P_2 to within the experimental accuracy. The reasons for choosing the results of figure 21 over the other measurements of P_2 were because the experimental error is much smaller than in the other cases, and because the internal consistency of the data of §§ 6 and 7, as indicated by the results of § 8, provides a basis for accepting the measurements.†

† After reading a draft of this paper Professor A. S. Lodge pointed out a method of determining the combination P_1+P_2. For torsional flow between parallel plates we find from (2.1) and (2.3) that

$$P_1(\dot{s}(R))+P_2(\dot{s}(R)) = \dot{s}(R)\,[\partial/\partial \dot{s}(R)]\,(p_{33}(0)-p_{33}(R)). \qquad (a)$$

At $r=0$ the stress is isotropic and $p_{33}(0)=p_{22}(0)$; moreover $p_{\mathrm{H}}=0$ in this flow (cf. § 8.1), so that the measurements of p_{22} made in apparatus IV can be applied to (a). For a free boundary at the rim of the apparatus we may take $p_{33}(R)=0$ (cf. (2.2)), but unfortunately measurements of this flow were made only with the sea-of-liquid configuration and so the term $\dot{s}(R)\,(\partial p_{33}(R)/\partial \dot{s}(R))$ must be included in (a). In spite of the fact that the data for $\bar{p}(0)$ are not detailed enough to adequately define a derivative, an estimate of P_1+P_2 has been made using (a). Neglecting the term in $p_{33}(R)$ we find that: at $\dot{s}=4.5\,\mathrm{s}^{-1}$, $P_2=-175\,\mathrm{dyn/cm^2}$; and at $\dot{s}=11.0\,\mathrm{s}^{-1}$, $P_2=570\,\mathrm{dyn/cm^2}$. Estimates of the term in $p_{33}(R)$ were made from the data for the cone-and-plate apparatus by a comparison of the measurements of $\bar{p}(R)$ for the free-boundary configuration with those for the sea-of-liquid configurations, and also from a

The measurements made by the Jackson & Kaye method do not agree with the results of figure 21, though it must be said that the experimental error associated with this method is quite large: at the highest shear rates the results are probably not accurate to within $\pm 1000\,\mathrm{dyn/cm^2}$. Moreover, it has recently been pointed out by Cowsley (1970) that the Jackson & Kaye method may be particularly sensitive to small departures of the flow field from the motion hypothesized for the cone-and-plate apparatus since the quantity $\partial F/\partial c$, needed to evaluate P_2 (see (2.12)), does not have a defined first derivative as $c \to 0$. Indeed an indication of this property can be seen from the experimental data by assuming that the measurements of P_1 and P_2 are known accurately, and that the total thrust $F(c)$ is correctly measured, then from the formulae (2.11) and (2.12) the function $\partial F/\partial c$ may be found. The outcome of such a procedure is shown in figure 27 for a particular angular velocity of the cone, and it should be noted that similar results are obtained for the other cone speeds. Also shown in figure 27 are the values of $\partial F/\partial c$ measured directly from the function $F(c)$ (cf. figure 24) and we see that these results give no indication of the expected singularity in $\partial^2 F/\partial c^2$ at $c = 0$. On the other hand, the resolution of this anomaly has,

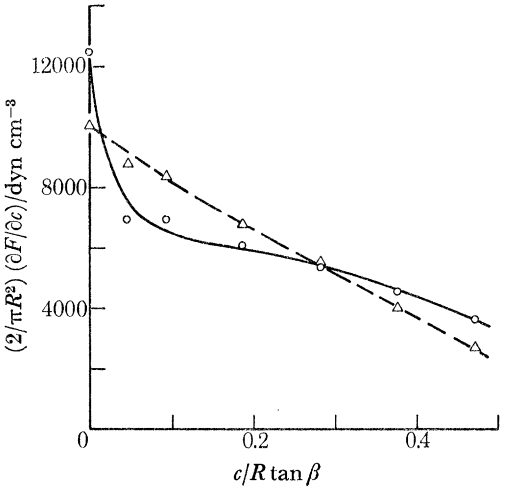

FIGURE 27. The quantity $\partial F/\partial c$ in the cone-and-plate apparatus plotted as a function of the gap width c, for $\Omega = 0.228\,\mathrm{s^{-1}}$. The shear rate at $c = 0$ is $4.23\,\mathrm{s^{-1}}$. – – – –, Determined directly from the measurements of $F(c)$; ——, determined from (2.11) and (2.12) on the assumption that P_1, P_2 and F have been correctly measured.

to date, been elusive: the effect of grinding off the tip of the cone would appear to be unimportant on the basis of the arguments presented in § 2.1, and because the results from the total-thrust measurements of apparatus I gave similar values of $\partial F/\partial c$ to those from the stress-distribution measurements of apparatus IV, in which the central area of the plate was excluded from consideration: the agreement between the results from apparatus I and apparatus IV, in which different boundary configurations at the rim were employed, would appear to rule out the influence of secondary flows near the rim as giving rise to the discrepancy; large scale secondary flows in the gap might be causing the anomalous results, but it is very difficult to estimate the

calculation of the kind described in appendix C. From these estimates it appears that the term $\dot{s}(\partial p_{33}(R)/\partial \dot{s})$ has a magnitude of about $150\,\mathrm{dyn/cm^2}$ at $\dot{s} = 4.5\,\mathrm{s^{-1}}$, and $350\,\mathrm{dyn/cm^2}$ at $\dot{s} = 11.0\,\mathrm{s^{-1}}$. Thus from (*a*) we deduce that $P_2 \approx -25\,\mathrm{dyn/cm^2}$ at $\dot{s} = 4.5\,\mathrm{s^{-1}}$, and $P_2 \approx 920\,\mathrm{dyn/cm^2}$ at $\dot{s} = 11.0\,\mathrm{s^{-1}}$; the corresponding values of P_2 from figure 21 are $-118\,\mathrm{dyn/cm^2}$ and $-20\,\mathrm{dyn/cm^2}$. The agreement between these two measurements is not very close, but the errors associated with the present computation could easily account for the differences. On the other hand, it is interesting that the trend, indicated in figure 21, towards positive values of P_2 at the higher shear rates is also reproduced in the present test.

influence of this source of error. In addition the observation discussed in appendix D gives results that are essentially in agreement with the measurements from the Jackson & Kaye method. These results were obtained by a method closely related to the Jackson & Kaye method, but one in which the quantity $\partial F/\partial c$ did not have to be evaluated.

The measurements by the Marsh & Pearson method are in agreement with the results of figure 21 only at the largest separation of the cone and the plate used in the test. Also the estimates of P_2 from the plate-and-plate apparatus, using the method of Kotaka *et al.*, are in fairly good agreement with the results of figure 21. Thus on the basis of these results it appears that the measurements of P_2 made at small values of $c/R\tan\beta$ differ substantially from the other, inherently more reliable, measurements of P_2, and that the large errors associated with the method render measurements virtually useless when using small values of $c/R\tan\beta$. On the other hand, the suggestion made by Cowsley (1970) of working with a re-entrant cone ($\beta < 0$) substantially reduces the errors and is probably the most reliable way of using the Marsh & Pearson method.

In view of the large amount of work involved in deducing P_2 by the methods discussed in § 9, and because of the difficulties encountered with these methods, it may be that the direct method of determining P_2 suggested in appendix A is worth further investigation.

10. In conclusion

In conclusion I shall briefly summarize the results of this set of measurements and discuss some of the impressions gained from the project.

The primary normal-stress difference was determined by three methods. Of these the normal force in the cone-and-plate apparatus and the stress-optical measurements gave values of P_1 which are in very good agreement, except at the higher shear rates where some experimental difficulties arose with the optical measurements. A method of resolving these difficulties was discussed and, by employing this method, extremely good agreement between both sets of data was attained over the whole range of the experiment. Similar agreement between the mechanical and the stress-optical measurements has been reported by Kaye *et al.* (1968), without the experimental difficulties encountered here, and it would appear that the combination of these two measurements provides a very useful experimental tool.

The value of P_1 obtained from measurements of the difference of the stress p_{22} across the gap of a pair of concentric cylinders did not agree with the other measurements of P_1 unless a hole-measuring error (p_H) was introduced. Taking this error into account the measurements from the concentric cylinders then showed good consistency with the other values of P_1 except for a small, apparently systematic, discrepancy at the lower shear rates which we are unable to explain. On the other hand, the discrepancy is such that it lies within the possible experimental error of the results. An interesting feature of the measurements in the concentric cylinders was that the quantity p_H was independent of the size of the hole in these experiments. This was unexpected in the light of some previous results of Broadbent (see Pritchard 1970) who made measurements with two different sized holes: the results were considered tentative at the time since one of the holes gave stress readings that differed significantly according to the direction of rotation of the cylinder, but since both these readings were smaller in magnitude than the reading obtained with the hole it was suggested that the size of the cavity may affect p_H. The present results indicate that this is not the case and thereby give warning that taking averages to eliminate small effects arising from asymmetries in a piece of equipment may be unreliable with nonlinear fluids.

PHILOSOPHICAL TRANSACTIONS OF THE ROYAL SOCIETY A MATHEMATICAL, PHYSICAL & ENGINEERING SCIENCES

The measurements of the distribution of the normal stress p_{22} made with apparatus IV, were used to determine the quantities $P_1 + 2P_2$ and p_H. A series of measurements in the cone-and-plate apparatus was made in which the cone angle and the boundary conditions at the rim were varied: the results suggest that these factors have little effect on the gradient $r(\partial\bar{p}/\partial r)$, except possibly in the case of the 5.67° cone at the highest shear rates. However, as Adams & Lodge (1964) were careful to point out, the axial movement of the rotating member may have an important influence on the results, especially at the lower cone angles. Adams & Lodge suggest that the amplitude of this movement should be less than about 5×10^{-6} cm, but a detailed investigation of its importance should be carried out, since even at the low amplitudes suggested it is possible that with the very viscous materials and with the small angled cones ($\beta \sim 1°$) employed some nonlinear processes may be operating which yield invalid results when averages are taken.

In order to analyse the data it was postulated that p_H is a function only of the shear rate of the undisturbed viscometric flow at the position of the hole. This proposition has not yet been proven theoretically but the results of a number of experimenters support it (except for a pathological example described by Pritchard (1970) which indicated a small influence of the shape of the cavity on p_H); indeed, for sharp-lipped, circular, holes the current experimental results and those of previous workers suggest that p_H is completely independent of the hole size, assuming that the cavity is deep and that the flows are sufficiently slow. The proposition has been proven for the case of a second-order fluid flowing past a two-dimensional slot, and an argument outlined in appendix A suggests how it could apply to a second-order fluid flowing past a circular hole. In the present experiments, with circular holes, the ratio p_H/P_1 appears to be about 0.16 (cf. figure 17). These results are in very good overall agreement with the theoretical predictions for the second-order-fluid model.

The measurements of the secondary normal-stress difference suggest that the methods of Jackson & Kaye and of Marsh & Pearson may give inaccurate values for P_2 coupled with large inherent experimental errors. The reasons for the anomalies observed in these experiments are not known, though it should be noted that they could arise either from non-ideal flows in the apparatuses or from a violation of the simple fluid assumptions. On the basis of the present experiments it would appear that the most reliable methods of determining P_2 are to use the normal-stress distribution $r(\partial\bar{p}/\partial r)$ in the cone-and-plate apparatus or the method of Kotaka *et al.* But, to avoid the need of relying on other data in order to measure P_2, direct methods of determining P_2 may prove to be the most attractive. For example the axial flow in the annulus between a pair of concentric cylinders (see Lodge 1964, p. 214) can be used to give a direct measurement of P_2, although there are a number of experimental difficulties in making the measurements and the computation of the results is rather complicated. Alternatively, the method proposed in appendix A avoids these experimental and computational difficulties, and accordingly it may be a useful way of determining P_2 directly.

I am indebted to the Science Research Council for support while at the University of Manchester Institute of Science and Technology, and to Professor R. B. Bird for support from his grants from the University of Wisconsin Graduate School and the Petroleum Fund of the American Chemical Society (Grant 1758-C).

In addition I should like to express my thanks to: Mr A. Lowe for his considerable help with the experiments; Dr A. Kaye for kindly making the birefringence measurements and for his helpful comments; Dr I. F. Macdonald for designing some modifications to the concentric cylinders

PHILOSOPHICAL TRANSACTIONS OF THE ROYAL SOCIETY A MATHEMATICAL, PHYSICAL & ENGINEERING SCIENCES

(apparatus VI); Professor A. S. Lodge for his suggestions and comments, and for his help in transporting a portion of the test liquid to Madison; Dr E. K. Harris, Jr. for making a series of measurements with the rheogoniometer at Madison; and Dr J. Meissner of B.A.S.F. (Ludwigshafen) for the gift of the polymer.

Appendixes

A. The intrinsic error in the use of a cavity to measure p_{22}

We consider a two-dimensional shear flow $u = \dot{s}y$, $\dot{s}$ being constant, above a surface whose upper boundary lies along the x-axis, as shown schematically in figure A 1. Puncturing this surface is a slot which opens into a larger cavity of extreme depth and at the bottom of which is a thin flexible diaphragm. In such a situation the stress near the diaphragm is isotropic and uniform and may therefore be balanced exactly by a pressure ($p_{-\infty}$) acting on the opposite side of the diaphragm, a pressure which returns the diaphragm to the position it occupied before the shear flow was generated. The difference between the stress p_{yy} acting on the surface $y = 0$ and the stress p_{yy} acting on the diaphragm ($= -p_{-\infty}$) is equal to the error introduced by this method of measurement. For a uniform shear flow, as considered here, the stress p_{yy} is the same throughout the undisturbed fluid, so that the measuring error is given by the difference between the stress p_{yy} far above the fixed surface and that near the bottom of the cavity. We shall call this error p_{H}. The upper surface driving the flow is assumed to be a large distance (i.e. many slot widths) above the fixed surface.

For slow flows of a Newtonian fluid past such a cavity the streamline patterns are necessarily symmetric about a plane passing through the centre of the hole and perpendicular to the flow. It follows immediately from a balance of forces, together with the symmetry of the stress distribution, that p_{yy} is constant along the centreline of the cavity, so that $p_{\mathrm{H}} = 0$. But with more complicated fluids the situation may be quite different for, even if the streamline pattern retains its symmetry, nonlinear contributions from the normal stresses will in general give rise to asymmetries in the shear stress p_{yx} about the plane through the centreline of the hole. A balance of forces now indicates that p_{yy} is not constant along the centreline of the cavity, thereby suggesting non-zero values for p_{H}.

Thus we shall assume, for simplicity, that the streamline patterns retain their symmetry for the more complicated fluids and that the 'memory effects' of the fluid are unimportant. These conditions apply, in particular, to the case of slow, two-dimensional, flows of a second-order fluid† (see Tanner 1966). Then, to exploit the symmetry of the flow field we introduce local coordinates based on the streamsurfaces of the flow, thereby preserving the symmetry of the stresses about the centreline of the hole.‡ It is convenient to use orthogonal coordinates (ξ_1, ξ_2, ξ_3)

† For sufficiently slow flows the second-order fluid is a valid approximation to any simple fluid (see Coleman & Noll 1960). For steady flows it has a constitutive relation, in Cartesian components, of the form (see Markovitz & Coleman 1964)

$$p_{ij} + p\delta_{ij} = \eta_0 e_{ij} + \beta_0 e_{ik} e_{kj} + \gamma_0 \left(v_p \frac{\partial e_{ij}}{\partial x_p} + e_{ip} \frac{\partial v_p}{\partial x_j} + e_{pj} \frac{\partial v_p}{\partial x_i} \right),$$

where $e_{ij} = (\partial v_i/\partial x_j + \partial v_j/\partial x_i)$ and v_i are the velocity components; p is an isotropic pressure; η_0, β_0, γ_0 are material parameters which are strictly constant over the range of validity of the approximation.

‡ Roughly speaking, the flow in the region near the centreline of the hole is similar to that generated by a cylinder rotating about its axis in a large expanse of fluid: that is, fluid particles move locally, in circular paths, the centres of which all lie on the centreline of the hole. Thus one may introduce a 'local' cylindrical-polar coordinate system based on the local curvature of the streamsurfaces. Then in the radial direction a balance of forces on a fluid element is given by (cf. Lodge 1964, pp. 190–192)

$$r\partial p_{22}/\partial r = p_{11} - p_{22}, \qquad \text{(i)}$$

in which the 1-direction is parallel to the fluid motion, the 2-direction is normal to the streamsurfaces, and the 3-direction forms the orthogonal triad; let h_1, h_2, h_3 be the 'scale factors' associated with these coordinates. Now the symmetry of the present problem requires that derivatives with respect to ξ_1 vanish on the centreline of the hole,† and using this condition in the stress equations of motion ($p_{ij,j} = 0$) we find in the 1- and the 2-directions respectively (e.g. see Happel & Brenner 1965, p. 489) that

$$\frac{\partial p_{21}}{\partial \xi_2} + \frac{2p_{21}}{h_1}\frac{\partial h_1}{\partial \xi_2} = 0, \tag{A 1}$$

and

$$\frac{\partial p_{22}}{\partial \xi_2} = (p_{11} - p_{22})\frac{1}{h_1}\frac{\partial h_1}{\partial \xi_2}. \tag{A 2}$$

Moreover, the symmetry of the flow field implies that the 2-direction lies along the centreline. Thus, using (A 1) to substitute for $h_1^{-1}(\partial h_1/\partial \xi_2)$ in (A 2) and integrating (A 2) along the centreline of the hole, we find that

$$p_{22}(\xi_2^T) - p_{22}(\xi_2^B)\,[= -p_{\mathrm{H}}] = -\frac{1}{2}\int_{\xi_2^B}^{\xi_2^T} \frac{p_{11} - p_{22}}{p_{21}}\frac{\partial p_{21}}{\partial \xi_2}\,\mathrm{d}\xi_2, \tag{A 3}$$

where ξ_2^T and ξ_2^B are the values of ξ_2 at the upper plate and at the bottom of the cavity respectively. If the line of integration passes through the centre of a vortex the present coordinate system is not applicable at that point. The integration must then be carried out in a piecewise manner. The expression (A 3) gives the intrinsic measuring error for any material in slow flows for which the streamline and stress patterns are symmetrical, in the way discussed above. In particular (A 3) applies to the case of a second-order fluid in which $(p_{11} - p_{22})$ is proportional to p_{21}^2: for such fluids the integral can be evaluated immediately and, when the hole is extremely deep so that the shear stress vanishes at ξ_2^B, we have that

$$p_{\mathrm{H}} = \tfrac{1}{4}(p_{11} - p_{22})_{\xi_2^T}. \tag{A 4}$$

This result is in agreement with the calculation of Tanner & Pipkin (1969).

If, on the other hand, the fluid flows over a circular hole, as opposed to the slot considered above, there will be a curvature of the streamsurfaces at the centre of the hole in the 1–3 plane. Assuming that the streamsurfaces are locally spherical at the centreline of the slot Higashitani & Pritchard (1971) have used similar arguments to those outlined above to suggest that p_{H}, for a second-order fluid, is approximately given by

$$p_{\mathrm{H}} = \tfrac{1}{6}(P_1 - P_2)_{\xi_2^T}, \tag{A 5}$$

where P_1 and P_2 are the primary and the secondary normal-stress differences respectively.

Finally, let us return to the geometrical configuration shown in figure A 1 and consider the experiment in which the upper plate is moved in a direction parallel to the direction of infinite extent of the slot. We shall assume that the flow is unidirectional and, although this condition

---

where r is the local radius of curvature of the streamlines and the 1- and 2-directions are defined in the same way as that described in the text. In the tangential direction the force balance yields

$$r\,\partial p_{21}/\partial r = -2p_{21}. \tag{ii}$$

Using (ii) to change the independent variable to p_{21} we may then integrate (i) along the centreline to yield the same result as that given in (A 4).

† If an applied pressure gradient is used to drive the flow an additional term, $h_1^{-1}(\partial p_{11}/\partial \xi_1)$ must be included in (A 1).

will be violated in general, experiments suggest that it is a good approximation to the actual flow (cf. Kearsley, unpublished experiments on flow along a square duct). Then to determine the intrinsic error in determining p_{22} in this example we base our coordinate system on the (continuous) surfaces of the flow field defined by the contours of constant velocity. The coordinates are then chosen in the same way as in the previous examples. Now the interesting feature of the present arrangement is that, for stable flows, the velocity field is symmetrically distributed about the centreplane of the slot irrespective of the properties of the material. Thus the symmetry arguments employed above no longer embody any restrictive assumptions about the kind of material under consideration; inertial effects however are again neglected.

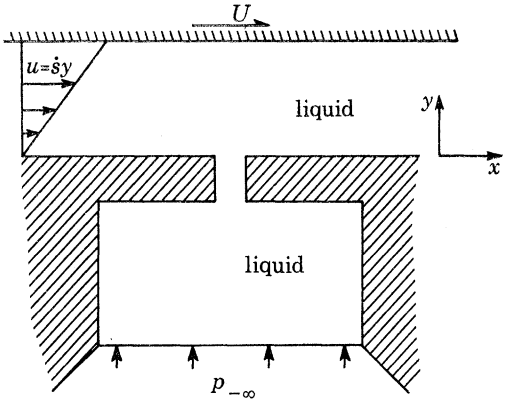

FIGURE A 1. Schematic arrangement of the method used to measure the stress p_{22}.

Accordingly the respective stress equations of motion in the 1- and 2-directions, at the centreline of the slot, are

$$\frac{\partial p_{21}}{\partial \xi_2} + \frac{p_{21}}{h_3}\frac{\partial h_3}{\partial \xi_2} = 0, \tag{A 6}$$

and

$$\frac{\partial p_{22}}{\partial \xi_2} = -(p_{22} - p_{33})\frac{1}{h_3}\frac{\partial h_3}{\partial \xi_2}. \tag{A 7}$$

In deducing these equations it has been assumed that the imposed pressure gradient $\partial p_{11}/\partial \xi_1 = 0$; the choice of the coordinate system ensures that the terms involving the other shear stresses do not enter (A 6) and (A 7). Thus, using (A 6) to eliminate h_3 from (A 7) and noting that $(p_{22} - p_{33})$ and p_{21} are functions only of the local shear rate in the material, we may change the independent variable from ξ_2 to p_{21}; then, on integrating along the centreline of the slot, we find that

$$p_{22}(P_{21}) - p_{22}(0)\,[= -p_{\mathrm{H}}] = \int_0^{P_{21}} \frac{p_{22} - p_{33}}{p_{21}}\,\mathrm{d}p_{21}. \tag{A 8}$$

The slot is assumed to be extremely deep so that the shear stress vanishes at the bottom; the shear stress at the upper surface is P_{21}. Differentiating (A 8) with respect to P_{21} we see that

$$P_{21}\,\mathrm{d}p_{\mathrm{H}}/\mathrm{d}P_{21} = -(p_{22} - p_{33})_{P_{21}}, \tag{A 9}$$

which provides a direct method of determining the secondary normal-stress difference. The above arguments are described in greater detail by Higashitani & Pritchard (1971).

B. The test used by Markovitz (1965*a*)

The test carried out by Markovitz (1965*a*) to check the consistency of his measurements was as follows:

(i) The primary normal-stress difference was determined from the difference in the normal stress p_{22} across the gap of a pair of concentric cylinders, as outlined in § 2.3.

(ii) The combination $P_1 + 2P_2$ was estimated from the gradient of the normal-stress distribution $p_{22}(r)$ in the cone-and-plate apparatus, as indicated in § 2.1.

(iii) Knowing P_1 and P_2, the distribution of the stress $p_{22}(r)$ in the plate-and-plate apparatus may be predicted from (2.16).

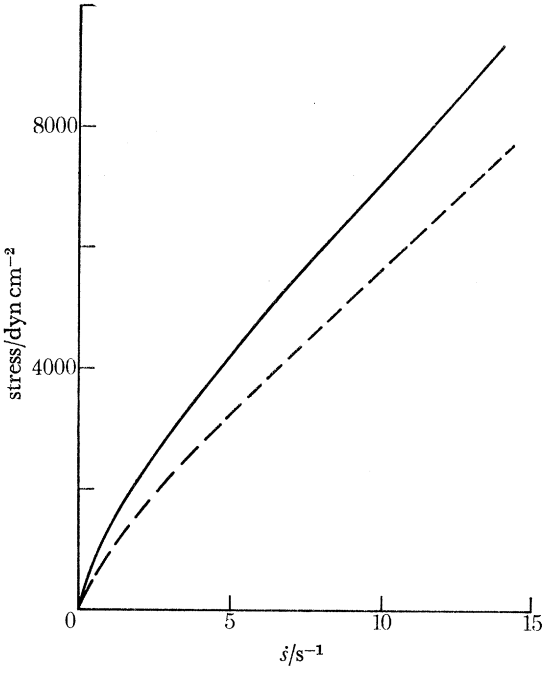

Figure B 1. A test of (2.16). ——, Supposed measurements of $p_{22}(\dot{s}) - p_{22}(0)$ using parallel plates with apparatus IV; – – –, the function

$$P_2(\dot{s}) + \int_0^{\dot{s}} (P_1 + P_2)\, \zeta^{-1} \mathrm{d}\zeta$$

determined from measurements in apparatus IV and apparatus VI.

From the measurements made in the present series of experiments we are able to repeat Markovitz's test. The value of P_1 chosen from the two sets of results for measurements in the concentric cylinders was that taken at $\kappa = 0.577$ (cf. figure 6). The function $P_1 + 2P_2$ from the cone-and-plate apparatus is shown in figure 11. From these two sets of data the distribution $p_{22}(r)$ in the plate-and-plate apparatus was deduced, and is indicated by the dashed line of figure B 1. The direct measurements of the stress distribution, taken from figure 14, are represented by the full line in figure B 1. The two curves do not agree in the present experiment.

C. The influence of the sea of liquid on $\bar{p}(R)$

In §§ 7 and 8 a number of experiments were discussed in which attempts were made to investigate the influence of the boundary conditions at the rim of the cone-and-plate apparatus. One interesting feature of the measurements of $\bar{p}(r)$ is shown in figure 10 from which it appears that $\bar{p}(r) = 0$ at a value of $r (= r_0)$ which is nearly independent of the shear rate. The same phenomenon was also observed with the 1.718° cone rotating in a sea of liquid, but with the 5.67° cone there was more variation in the value of r_0 than in the other two cases. When using the free-boundary condition there was also more variation in the value of r_0 than that shown in figure 10. In this appendix we shall try to give a rough quantitative account of this phenomenon for the sea-of-liquid experiments.

From the theory of § 2.1 it follows for the cone-and-plate apparatus that

$$p_{22}(r) = P_2 + (P_1 + 2P_2) \ln (r/R). \tag{C 1}$$

But the stress $\bar{p}(R)$ actually measured differs from P_2 because of contributions arising from the hole-measuring error p_H, the Weissenberg effect in the sea of liquid (which we shall call p_W) and from unwanted flow conditions such as secondary flows. The latter effects are neglected in the present calculations. Thus we have that (cf. (7.1))

$$-p_{22} = \bar{p} + p_H - p_W. \tag{C 2}$$

Then on substituting (C 2) in (C 1) it follows that $\bar{p}(r) = 0$ when

$$\ln (r_0/R) = -(P_2 + p_H - p_W)/(P_1 + 2P_2). \tag{C 3}$$

To estimate the quantity p_W we shall assume that it is equal to the normal stress exerted on the wall of a long cylinder rotating about its own axis in a fluid of large radial extent. In effect we are saying that the boundary condition (2.2), namely $p_{33}(R) = 0$, is not valid for the sea of liquid configuration and should be replaced by the condition $p_{33} = p_W$, where p_W arises from the fluid flow in the region $r > R$. A good approximation to p_W may be obtained from (2.22) by using power-law relations to describe the material properties. Thus if $P_1 = A p_{21}^B$ and $\dot{s} = \mathscr{A} p_{21}^{\mathscr{B}}$ it follows from (2.22) that

$$p_W = (1/2B)\, P_1(\dot{s}_W), \tag{C 4}$$

where $\dot{s}_W$ is the shear rate at the wall of our hypothetical cylinder. Now, because of the power-law relations, $\dot{s}_W$ may be related to the shear rate $\dot{s}$ in the gap of the cone-and-plate apparatus. From (2.3) we find that

$$\dot{s}_W/\dot{s} = 2\mathscr{B} \tan \beta, \tag{C 5}$$

and again, by virtue of the power-law relation, $P_1(\dot{s}_W)$ may be written in terms of $P_1(\dot{s})$, in consequence of which

$$\begin{aligned} p_W &= (1/2B)\, (2\mathscr{B} \tan \beta)^{B/\mathscr{B}}\, P_1(\dot{s}) \\ &= \{\phi(\beta)/2B\}\, P_1(\dot{s}), \quad \text{say.} \end{aligned} \tag{C 6}$$

Then, putting $p_H/P_1 = \lambda$, (C 3) becomes

$$\ln (r_0/R) = -(P_2/P_1 + \lambda - \phi(\beta)/2B)/(1 + 2P_2/P_1). \tag{C 7}$$

From (C 7) we now see that if λ is nearly constant and if $P_2/P_1 \ll 1$ (both of which are applicable in the present case) the quantity $\ln (r_0/R)$ is nearly independent of the shear rate $\dot{s}$. On the other hand, (C 7) depends upon the cone angle β, as suggested above, and using the appropriate values of B $(= 1.98)$ and $\mathscr{B} (= 2.65)$, for the present experiments, we can obtain a rough estimate of the

dependence of ln (r_0/R) on β. For the purposes of this computation we shall assume that $P_2/P_1 = 0$ and that $\lambda = 0.16$ (cf. figure 17). The results are shown in table C 1, and in view of the approximations involved, they are thought to be remarkably close to the observed values of ln (r_0/R), thereby supporting to some extent the discussion of §§ 7 and 8.

TABLE C 1

β	$\phi(\beta)/2B$	$\lambda - \phi(\beta)/2B$	observation $-\ln(r_0/R)$
1.72°	0.0545	0.1055	~0.07
3.27°	0.0948	0.0652	0.043
5.62°	0.1404	0.0196	0.03–0.007

D. AN ESTIMATE OF THE SECONDARY NORMAL-STRESS DIFFERENCE

In the course of the experiments in which P_2 was determined by the Jackson & Kaye method (§ 9.1) it was observed, for small non-zero values of $c/R \tan\beta$, that to a very good approximation the measured stress $\bar{p}$ varies logarithmically with the radius over a large extent of the plate. In § 7 we described how the expected logarithmic distribution of $\bar{p}$ is observed when $c/R \tan\beta = 0$.

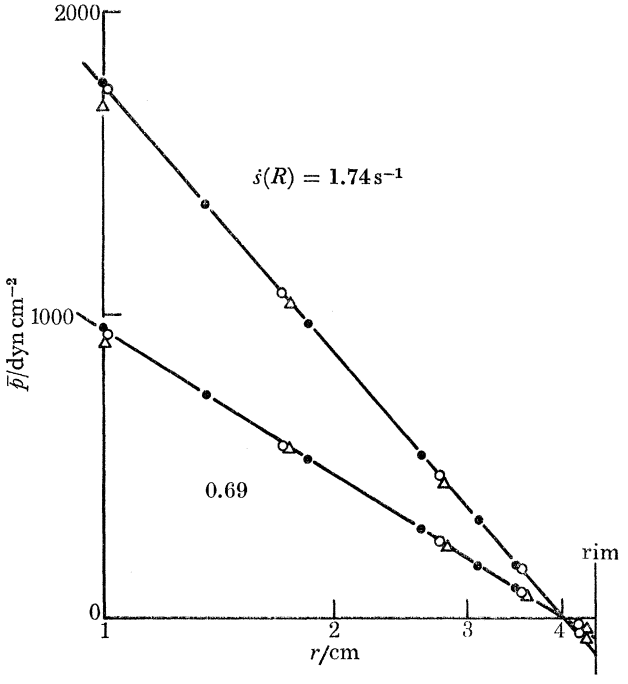

FIGURE D 1. The normal-stress distribution $\bar{p}(r)$ in a cone-and-plate apparatus for various values of c with the restriction that $\dot{s}(R) =$ constant. The measurements were made on apparatus IV with the sea-of-liquid configuration. $R = 4.41$ cm; $\beta = 3.27°$. ●, $c/R \tan\beta = 0$; ○, $c/R \tan\beta = 0.025$; △, $c/R \tan\beta = 0.051$.

However, in figure D 1 it is seen, with $c/R \tan\beta = 0.025$, that $\bar{p}$ is well represented by a logarithmic distribution over the radial extent of the measurement; indeed, even when $c/R \tan\beta = 0.051$, it is only the innermost point which deviates from the logarithmic distribution. Moreover the results of figure D 1 indicate that not only is the distribution of $\bar{p}$ very nearly logarithmic, but, by adjusting the angular velocity Ω so that $\dot{s}(R)$ is the same for each value of $c/R \tan\beta$, all the values of $\bar{p}$ are

closely represented by a common curve. We have used this observation to make another estimate of P_2.

From the assumption (7.1) it follows that the normal force F acting on the plate may be separated into two components $\bar{F}$ and f corresponding to the stresses $\bar{p}$ and p_{H} respectively. Thus we have that

$$F = \bar{F} + f. \tag{D 1}$$

Let us now carry out the experiment in which Ω is held constant, and the cone and the plate are separated by an amount Δc from the position $c = 0$. The normal force F thereby changes, to first order in Δc, by an amount $(\partial F/\partial c)\,\Delta c$. If now, at the separation Δc, we adjust the speed of rotation by an amount $\Delta\Omega$, the change in the normal force is given approximately by $(\partial F/\partial\Omega)_{\Delta c}\,\Delta\Omega$ and it follows from (D 1) that

$$\left(\frac{\partial F}{\partial c}\right)_{c=0}\Delta c + \left(\frac{\partial F}{\partial \Omega}\right)_{c=\Delta c}\Delta\Omega = \left(\frac{\partial \bar{F}}{\partial c}\right)_{c=0}\Delta c + \left(\frac{\partial \bar{F}}{\partial \Omega}\right)_{c=\Delta c}\Delta\Omega + \left(\frac{\partial f}{\partial c}\right)_{c=0}\Delta c + \left(\frac{\partial f}{\partial \Omega}\right)_{c=\Delta c}\Delta\Omega. \tag{D 2}$$

The deduction made from the results of figure (D 1) is that, when $\dot{s}(R)$ is held constant, the sum $(\partial\bar{F}/\partial c)_{c=0}\Delta c + (\partial\bar{F}/\partial\Omega)_{c=\Delta c}\Delta\Omega$ may be equated to zero, to within the experimental error. Since $\dot{s}(R)$ is a constant, the quantities Δc and $\Delta\Omega$ are related by means of (2.3) and we have that

$$\Delta\Omega = \{\dot{s}(R)/R\}\,\Delta c. \tag{D 3}$$

Equation (D 2) accordingly reduces to

$$\left(\frac{\partial F}{\partial c}\right)_{c=0} + \frac{\dot{s}(R)}{R}\left(\frac{\partial F}{\partial \Omega}\right)_{c=\Delta c} = \left(\frac{\partial f}{\partial c}\right)_{c=0} + \frac{\dot{s}(R)}{R}\left(\frac{\partial f}{\partial \Omega}\right)_{c=\Delta c}. \tag{D 4}$$

In (D 4) the quantity $(\partial F/\partial c)_{c=0}$ is already known as a function of P_1 and P_2 from (2.11); the term containing $(\partial F/\partial\Omega)_{c=\Delta c}$ may similarly be written as a function of P_1 and P_2, and from (2.10) we have that

$$\frac{\partial F}{\partial \Omega} = -\pi\int_R^R \left[2r\frac{\mathrm{d}P_2}{\mathrm{d}\dot{s}} - (r^2 - R_{\mathrm{i}}^2)\left(\frac{\tan\beta}{c + r\tan\beta}\frac{\mathrm{d}P_2}{\mathrm{d}\dot{s}} + \frac{1}{r}\left(\frac{\mathrm{d}P_1}{\mathrm{d}\dot{s}} + \frac{\mathrm{d}P_2}{\mathrm{d}\dot{s}}\right)\right)\right]\frac{\mathrm{d}\dot{s}}{\mathrm{d}\Omega}\,\mathrm{d}r, \tag{D 5}$$

where $\dot{s}$ and Ω are related by (2.3). If we now make the assumption that $\mathrm{d}P_1/\mathrm{d}\dot{s}$ and $\mathrm{d}P_2/\mathrm{d}\dot{s}$ are both constants over the range of integration it becomes a simple matter to evaluate (D 5). (For small values of $c/R\tan\beta$ this assumption is nearly satisfied (cf. figures 6, 21 (a)), especially at the higher shear rates). Accordingly $(\partial F/\partial\Omega)$ takes the form

$$\frac{1}{\pi}\frac{\partial F}{\partial \Omega} = \Gamma_1\frac{\mathrm{d}P_1}{\mathrm{d}\dot{s}} + \Gamma_2\frac{\mathrm{d}P_2}{\mathrm{d}\dot{s}}, \tag{D 6}$$

where Γ_1 and Γ_2 are determined by the geometric quantities R_{i}, R, c, β, Ω. Following similar arguments, together with the assumption that $\mathrm{d}p_{\mathrm{H}}/\mathrm{d}\dot{s}$ is constant over the range of integration, we find that the terms on the right-hand side of (D 4) may be expressed as

$$\frac{1}{\pi}\frac{\partial f}{\partial c} = -\gamma_1\frac{\mathrm{d}p_{\mathrm{H}}}{\mathrm{d}\ln\dot{s}}, \quad \frac{1}{\pi}\frac{\partial f}{\partial \Omega} = \gamma_2\frac{\mathrm{d}p_{\mathrm{H}}}{\mathrm{d}\dot{s}}, \tag{D 7}$$

where γ_1 and γ_2 are also determined by the geometric properties of the apparatus. Then on substituting the various terms in (D 2) we find that

$$P_2(\dot{s}) = -\left(1 + \frac{\Gamma_1\tan\beta}{(R - R_{\mathrm{i}})^2}\right)\frac{\mathrm{d}P_1}{\mathrm{d}\ln\dot{s}} + \frac{(\gamma_1 R - \gamma_2)\tan\beta}{(R - R_{\mathrm{i}})^2}\frac{\mathrm{d}p_{\mathrm{H}}}{\mathrm{d}\ln\dot{s}} + \left(\frac{2R_{\mathrm{i}}}{R - R_{\mathrm{i}}} - \frac{\Gamma_2\tan\beta}{(R - R_{\mathrm{i}})^2}\right)\frac{\mathrm{d}P_2}{\mathrm{d}\ln\dot{s}}, \tag{D 8a}$$

which for convenience we shall write as

$$P_2(\dot{s}) = -K_1\frac{\mathrm{d}P_1}{\mathrm{d}\ln\dot{s}} + K_2\frac{\mathrm{d}p_\mathrm{H}}{\mathrm{d}\ln\dot{s}} + K_3\frac{\mathrm{d}P_2}{\mathrm{d}\ln\dot{s}}. \qquad (\mathrm{D}\,8b)$$

TABLE D 1

$\dot{s}$	$\Delta c/R\tan\beta$	K_1	$\frac{\mathrm{d}P_1/\mathrm{d}\ln\dot{s}}{\mathrm{dyn\,cm^{-2}}}$	K_2	$\frac{\mathrm{d}p_\mathrm{H}/\mathrm{d}\ln\dot{s}}{\mathrm{dyn\,cm^{-2}}}$	K_3	$\frac{P_2}{\mathrm{dyn\,cm^{-2}}}$
11.00	0.004	0.330	4575	0.394	579	0.391	−1340
	0.040	0.363		0.720		0.318	−1238
1.74	0.004	0.330	957	0.394	103	0.391	−275
	0.040	0.363		0.720		0.318	−274
0.69	0.004	0.330	564	0.394	90	0.391	−151
	0.040	0.363		0.720		0.318	−140

Since $K_{1,2,3}$ are $O(1)$ and since the quantity $(\mathrm{d}P_2/\mathrm{d}\ln\dot{s})$ is expected to be much smaller than the other terms of (D 8*b*) we shall neglect the last term of this equation, and P_2 may be found directly from (D 8*b*). Some estimates of P_2, thus computed, are shown in table D 1; the constants K_1, K_2, K_3 have been evaluated for the geometric properties of the apparatus in which the results of figure D1 were obtained.

The values of P_2 shown in the table are in agreement with the results found from the Jackson & Kaye method, whereas in this case we have not had to evaluate the slope $(\partial F/\partial c)_{c=0}$ from experimental data.

Since $\mathrm{d}P_2/\mathrm{d}\dot{s}$ appears to be negative the effect of the neglected terms would be to increase the magnitude of P_2. The influence of the sea of liquid, which was used in these experiments, has been neglected in the computations in the belief that it would have a negligible influence on the results.

REFERENCES

Adams, N. & Jackson, R. 1967 A trifilar-suspension rheogoniometer. *J. Scient. Instrum.* **44**, 461.

Adams, N. & Lodge, A. S. 1964 Rheological properties of concentrated polymer solutions. II. A cone-and-plate and parallel-plate pressure distribution apparatus for determining normal stress differences in steady shear flow. *Phil. Trans. R. Soc. Lond.* A **256**, 149.

Broadbent, J. M. & Lodge, A. S. 1971 Determination of normal stress differences in steady shear flow. III. A wide-gap concentric cylinder apparatus. *Rheology Research Center, Madison, Wis. Rep.* no. 6.

Chandrasekhar, S. 1961 *Hydrodynamic and hydromagnetic stability*. Oxford University Press.

Coleman, B. D., Markovitz, H. & Noll, W. 1966 *Viscometric flows of non-Newtonian fluids*. Berlin: Springer Verlag.

Coleman, B. D. & Noll, W. 1959 On certain steady flows of general fluids. *Archs ration. Mech. Analysis* **3**, 289.

Coleman, B. D. & Noll, W. 1960 An approximation theorem for functionals with applications in continuum mechanics. *Archs ration. Mech. Analysis* **6**, 355.

Cowsley, C. W. 1970 Improvements to total thrust methods for the measurement of second normal stress differences. University of Cambridge, Dept. of Chem. Engrg. Polymer Processing Res. Centre, *Rep.* no. 6.

Greensmith, H. W. & Rivlin, R. S. 1953 The hydrodynamics of non-Newtonian fluids. III. The normal stress effect in high polymer solutions. *Phil. Trans. R. Soc. Lond.* A **245**, 399.

Griffiths, D. F. & Walters, K. 1970 On edge effects in rheometry. *J. Fluid Mech.* **42**, 379.

Happel, J. & Brenner, H. 1965 *Low Reynolds number hydrodynamics*. New York: Prentice Hall.

Harris, E. K., Jr. 1970 Viscometric properties of polymer solutions and blends as functions of concentration and molecular weight. Ph.D. dissertation, University of Wisconsin (Madison).

Higashitani, K. & Pritchard, W. G. 1971 A kinematic calculation of intrinsic errors in pressure measurements made with holes. (*sub judice.*)

Jackson, R. & Kaye, A. 1966 The measurement of the normal stress differences in a liquid undergoing simple shear flow using a cone-and-plate total thrust apparatus only. *Br. J. appl. Phys.* **17**, 1355.

Janeschitz-Kriegl, H. 1969 Flow birefringence of elastico-viscous polymer systems. *Adv. Polymer Sci.* **6**, 170.

Kaye, A. 1965 Flow problems with rheological equations of state. D.Phil. dissertation, University of Oxford.

PHILOSOPHICAL TRANSACTIONS OF THE ROYAL SOCIETY A MATHEMATICAL, PHYSICAL & ENGINEERING SCIENCES

Kaye, A., Lodge, A. S. & Vale, D. G. 1968 Determination of normal stress differences in steady shear flow. *Rheologica Acta* **7**, 368.

Kaye, A. & Saunders, D. W. 1964 A concentric cylinder viscometer for the measurement of flow birefringence and viscosity in concentrated polymer solutions. *J. scient. Instrum.* **41**, 139.

Kotaka, T., Kurata, M. & Tamura, M. 1959 Normal stress effect in polymer solutions. *J. appl. Phys.* **30**, 1705.

Lipson, J. M. & Lodge, A. S. 1968 Determination of normal stress differences in steady shear flow. I. Stability of a polyisobutene liquid. *Rheologica Acta* **7**, 364.

Lodge, A. S. 1960 The isotropy of Gaussian molecular networks and the stress birefringence relations for rubber-like materials cross-linked in stressed states. *Kolloid Z.* **171**, 46.

Lodge, A. S. 1964 *Elastic liquids*. New York: Academic Press.

Lodge, A. S. & Stark, J. H. 1970 On the description of rheological properties of viscoelastic continua, II. Proof that Oldroyd's 1950 formalism includes all 'simple fluids'. *Rheology Research Center, Madison, Wis. Rep.* no. 5.

Markovitz, H. 1965*a* The normal stress effect in steady torsional flow, predicted and experimental results. *Phys. Fluids* **8**, 200.

Markovitz, H. 1965*b* Normal stress functions from Couette flow measurements. *J. Polymer Sci.* B **3**, 3.

Markovitz, H. & Coleman, B. D. 1964 Incompressible second-order fluids. *Adv. appl. Mech.* **8**, 69.

Marsh, B. D. & Pearson, J. R. A. 1968 The measurement of normal-stress differences using a cone-and-plate total thrust apparatus. *Rheologica Acta* **7**, 326.

Noll, W. 1958 A mathematical theory of the mechanical behaviour of continuous media. *Archs ration. Mech. Analysis* **2**, 197.

Oldroyd, J. G. 1950 On the formulation of rheological equations of state. *Proc. R. Soc. Lond.* A **200**, 523.

den Otter, J. L. 1967 Dynamic properties of some polymeric systems. Doctoral dissertation. University of Leyden.

Pearson, J. R. A. 1967 The lubrication approximation applied to non-Newtonian flow problems: A perturbation approach. In *Non-linear partial differential equations* (ed. W. F. Ames). New York: Academic Press.

Philippoff, W. 1964 Streaming birefringence of polymer solutions. *J. Polym. Sci.* C **5**, 1.

Pipkin, A. 1968 Controllable viscometric flows. *Q. Jl appl. Math.* **26**, 87.

Pritchard, W. G. 1970 The measurement of normal stresses by means of liquid-filled holes in a surface. *Rheologica Acta* **9**, 200.

Tanner, R. I. 1966 Plane creeping flows of incompressible second-order fluids. *Phys. Fluids* **9**, 1246.

Tanner, R. I. & Pipkin, A. 1969 Intrinsic errors in pressure-hole measurements. *Trans. Soc. Rheol.* **13**, 471.

Thomas, R. H. & Walters, K. 1964*a* The stability of elastico-viscous flow between rotating cylinders. Part 1. *J. Fluid Mech.* **18**, 33.

Thomas, R. H. & Walters, K. 1964*b* The stability of elastico-viscous flow between rotating cylinders. Part 2. *J. Fluid Mech.* **19**, 557.

Walters, K. & Waters, N. D. 1968 On the use of a rheogoniometer; part I—steady shear. From *Polymer systems: deformation and flow* (ed. R. E. Wetton & R. W. Whorlow), p. 211. London: Macmillan.

Zimm, B. H. 1956 Dynamics of polymer molecules in dilute solution: viscoelasticity, flow birefringence and dielectric loss. *J. chem. Phys.* **24**, 269.

PHILOSOPHICAL TRANSACTIONS OF THE ROYAL SOCIETY A MATHEMATICAL, PHYSICAL & ENGINEERING SCIENCES